NOTICE

The quality of this microform is heavily dependent upon the quality of the original thesis submitted for microfilming. Every effort has been made to ensure the highest quality of reproduction possible.

If pages are missing, contact the university which granted the degree.

Some pages may have indistinct print especially if the original pages were typed with a poor typewriter ribbon or if the university sent us an inferior photocopy.

Reproduction in full or in part of this microform is governed by the Canadian Copyright Act, R.S.C. 1970, c. C-30, and subsequent amendments.

AVIS

La qualité de cette microforme dépend grandement de la qualité de la thèse soumise au microfilmage. Nous avons tout fait pour assurer une qualité supérieure de reproduction.

S'il manque des pages, veuillez communiquer avec l'université qui a conféré le grade.

La qualité d'impression de certaines pages peut laisser à désirer, surtout si les pages originales ont été dactylographiées à l'aide d'un ruban usé ou si l'université nous a fait parvenir une photocopie de qualité inférieure.

La reproduction, même partielle, de cette microforme est soumise à la Loi canadienne sur le droit d'auteur, SRC 1970, c. C-30, et ses amendements subséquents.

GAS AND VAPOR PERMEATION THROUGH POLYMER MEMBRANES

Xianshe Feng

A THESIS

SUBMITTED TO THE SCHOOL OF GRADUATE STUDIES

IN PARTIAL FULFILLMENT OF THE REQUIREMENTS

FOR THE DEGREE OF

MASTER OF APPLIED SCIENCE

IN THE DEPARTMENT OF CHEMICAL ENGINEERING

UNIVERSITY OF OTTAWA

May 1990

ISBN 0-315-68092-X

UNIVERSITÉ D'OTTAWA
UNIVERSITY OF OTTAWA

Abstract

The permeation data of CO_2/CH_4 mixtures through cellulose acetate membranes were analyzed. The pore flow model initially used for pure gas permeation was extended to the permeation process of gas mixtures. The permselectivity calculated using the model was compared with the experimental data, and the results showed the applicability of the model to the description of gas mixture permeation process. The effects of feed composition, operating pressure and the pore size of the membrane on the permeability and selectivity of the membrane were determined and interpreted on the basis of the pore flow model.

The separation of organic vapors from air was attempted by means of polyimide membranes at ambient temperature. The membranes were prepared by a phase inversion technique and then dried using a solvent exchange method. The experimental results show that the permselectivity depended on the porous structure of the membrane which can be controlled by the membrane making conditions. The effects of several parameters involved in the procedure for membrane preparation on membrane performance were determined.

Acknowledgements

The author is extremely grateful to Dr. S. Sourirajan and Dr. T. Matsuura for their indispensable guidance, direction and encouragement throughout the course of the work, and also to Dr. H. Tezel for her precious discussions.

He wishes to thank Mr. Y. Chen for providing the CO_2 and CH_4 permeability data.

The author gratefully acknowledges the financial support given to this project by Shell Canada – Oakville Research Centre and also NSERC through their grants to the Industrial Membrane Research Institute (IMRI), associated with the Department of Chemical Engineering.

The valuable assistance and the kind consideration of the people in the Department of Chemical Engineering and IMRI are much appreciated.

Nomenclature

A	membrane area, m^2
$\bar{c}$	mean speed of gas molecules, m/s
d	collision diameter of gas molecules, m
J	membrane thickness-normalized permeability, $mol/m^2.s.Pa$
K	constant in Eq.(3.5), Pa^{-1}
k	constant in Eq.(3.5), $ln(Pa.s).Pa^{-1}$
k_H	Henry's constant, $mol/m^3.Pa$
l	effective membrane thickness, m
M_i	molecular weight of gas i
N	Avogadro number
N_t	number of pores on per unit membrane area, m^{-2}
P	membrane permeability, $mol.m/m^2.s.Pa$
p	pressure, Pa
$p_{h,i}$	partial pressure of component i on feed side, Pa
$p_{l,i}$	partial pressure of component i on permeate side, Pa
p_m	average pressure, Pa
Δp	pressure difference across the membrane, Pa
Δp_i	difference in partial pressure of gas i across the membrane, Pa
$[PR]_i$	permeation rate of gas i defined by Eq.(2.1), mol/s

Q_K permeation flux by Knudsen flow mechanism, mol/m^2.s

Q_S permeation flux by surface flow mechanism, mol/m^2.s

Q_{Slip} permeation flux by slip flow mechanism, mol/m^2.s

Q_t total permeation flux through membrane, mol/m^2.s

Q_V permeation flux by viscous flow mechanism, mol/m^2.s

q_s gas transport rate through a single pore by surface flow, mol/s

r pore radius, m

$[SF]$ separation factor

T temperature, K

t thickness of adsorbed gas layer, m

u velocity of adsorbed gas layer movement, m/s

V volumetric permeation rate of air, ml/min

W_t Weight of LiCl leached in gelation bath at time t, g

W_∞ value of W_t at the time when LiCl leaching has practically ceased, g

X_i mole fraction of component i on feed side

Y_i mole fraction of component i on permeate side

Greek Letters:

α selectivity of membrane

δ solubility parameter, (cal/cm^3)$^{1/2}$

η coefficient of viscosity of gas, Pa.s

λ mean free path of gases, m

μ surface viscosity of adsorbed gas layer, Pa.s

ϕ spreading pressure, N/m

ψ the ratio of gas molecule size and pore size

Table of Contents

List of Tables

List of Figures

Chapter 1

Introduction

1.1 General

With the growing demands for better separation and/or purification methods in chemical, petroleum, biological and other processes, membrane technology has been attracting more and more attention. The great interest in membrane separation technology lies mainly in the fact that it is potentially energy–efficient. Membrane–based technology has emerged as an important unit operation in chemical engineering separations.

Although the concept of membrane separation dates back to last century, only recently have membrane processes became economically competitive. In general, there are two types of problems (Ward, 1986). First, the separation ability and the production capacity of the early membranes were completely inadequate for commercially attractive processes. Second, the fragility of thin polymer membranes has made it difficult to build reliable systems that work for a long time under practical operating conditions.

For the last three decades, many efforts have been devoted to the research and development of membrane processes, and several key technical breakthroughs have been made. Nowadays, membrane separations have evolved into an expanding and diverse field, including ultrafiltration (UF), reverse osmosis (RO), gas separation, and pervaporation. Their development status can be seen from Figure 1.1 (Zhu and Liu, 1988). In comparison with the industrialized processes such as dialysis, UF and RO, gas separation by means of membrane is growing most rapidly towards the technical maturity.

1.2 Membrane Gas Separation

The concept of gas separation by membrane is not new. In as early as 1831 it was recorded that the escape rates of ten gases from natural rubber balloons are different. Thirty years later, Graham studied gas permeation through natural rubber and demonstrated that the natural rubber could achieve oxygen enrichment of air (Stanley, 1986).

Despite the early recognition of the separation potential of membranes, their industrial application for the separation of gas mixtures is only more than ten years old. During the intervening period, much work has been done that widened the research scope to many gases and a variety of polymers. The possibilities of several gas separations by membranes became apparent, but the early attempts to realize them failed because of low fluxes of the membranes at that time. With the invention of asymmetric membranes for liquid phase separation process, namely reverse osmosis, the door was opened for the rapid advance in membrane gas separation field.

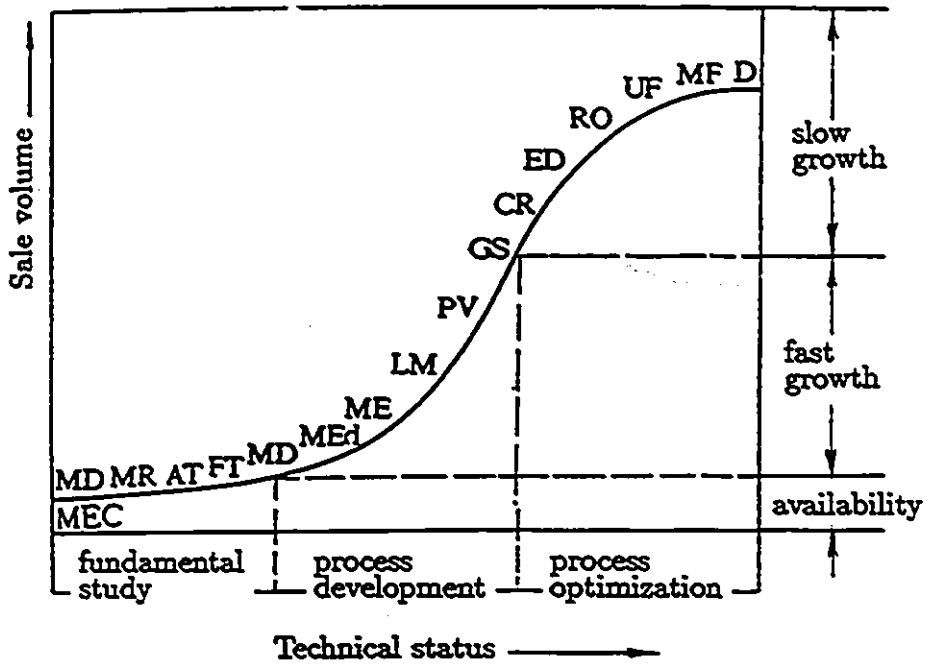

Figure 1.1: The development status of membrane processes. D–dialysis, MF–microfiltration, UF–ultrafiltration, RO–reverse osmosis, ED–electrodialysis, CR–controlled release, GS–gas separation, PV–pervaporation, LM–liquid membrane, ME–membrane electrodes, MEd–membrane electrolyzers, MD–membrane medical devices, FT–faciliated transport, AT–active membranes, MR–membrane reactor, MEC–membrane energy conversion system (Zhu and Liu, 1988).

1.2.1 Technical Advance

During the past 30 years, substantial work has been done on membrane gas separation, and many technical breakthroughs came out. They include but not limited to

- In the early 1960s, Loeb and Sourirajan made the first asymmetric cellulose acetate membrane for reverse osmosis (Sourirajan, 1970). This invention is a milestone in leading to today's membrane separation advance, and contributes directly to the commercial gas separation by membranes.

- In the later 1960s, the dry Loeb-Sourirajan membrane suitable for gas separation was made successfully (Vos and Burris, 1969; Gantzel and Merten, 1970).

- In the middle 1970s, Ward and coworkers (1976) developed an approach for producing an ultrathin membrane of block copolymer by a Langmuir-Blodgett technique.

- In 1979, Henis and Tripodi (1980a,b, 1981) invented the resistance-model type of hollow fiber membrane, which has been introduced to market as PRISM separator by Monsanto Company. Now, more than 1000 PRISM separators are in operation throughout the world (Baldus and Tillman, 1986), which, maybe more than anything else, indicates that membrane gas separation as a unit operation has come of age.

- Recently, Ube Industries marketed asymmetric polyimide membrane separators, which are highly resistant to heat and contaminates (Hakuta et al., 1987).

- In June 1989, a breakthrough in the separation of oxygen and nitrogen was reported (Generon, 1989). This new system, called Generon HP, is believed to

be the latest and the most advanced air separation module ever produced.

1.2.2 Applications

Membrane gas separation has been applied to many processes with commercial success. Of great interest are processes such as

a) H_2 recovery

b) CO_2 recovery

c) O_2 enrichment and N_2 production from air, etc.

Most of the applications are directed to hydrogen recovery from various industrial gas streams, such as ammonia and methanol synthesis purges, catalytic cracker, hydrocracker and hydrogenator purges. Membrane can also be used to adjust the N_2/H_2 ratio in ammonia synthesis and H_2/CO ratio in syngas production (Laverty and O'Hair, 1986; MacLean et al., 1980).

A number of membrane systems separating CO_2 are used in enhanced oil recovery (Schendel, 1986), natural gas sweeting (Mazur and Chan, 1982), and landfill gas upgrading (Ruf and Egli, 1988).

Recently, much attention has been paid to O_2/N_2 separation. Membranes that are able to achieve an oxygen enrichment of 40% concentration from air have been commercialized for medical use. More attractively, O_2 enriched air can be utilized in a furnace to improve combustion, and also in the liquification and gasification of coal to produce suitable process gases (Laverty and O'Hair, 1986). N_2 can be used as an inert purge for storage and shipment of flammable liquids throughout chemical industry. Moreover, N_2 rich air for the blanketing of foods and vegetables provides a nontoxic, nonresidual protection.

Separating organic vapor from the contaminated air is another interesting application (Strathmann et al., 1986). In addition to the loss of valuable solvents, organic emissions present severe health, safety and environmental problems. Membrane can be used to remove and recover these vapors. Nippon Kokan (1987) markets a membrane system for gasoline vapor recovery.

There are several other areas to which suitable membranes can be utilized such as helium recovery from natural gas and deep-sea diving atmosphere, dehydration of process gases, and acid gas treatment (Pan and Habgood, 1978b; Stern, 1986).

1.2.3 Characteristics

Membrane gas separation has many advantages over the conventional processes such as absorption, adsorption and cryogenic. Compactness, flexibility and simplicity are three of the strongest points (MacLean, 1986).

Membrane units are modular in construction. There is no significant economy of scale so they can be utilized in either large or small processing capacity. It is easy to add more modules for plant enlargement, or replace them if necessary, without much change of the overall process scheme. Membrane installations usually require less space than conventional processes. This point is very important when space is at a premium. Having no moving parts, the start-up and operation is rather straightforward, and minimal operator attention or computer intervention is needed.

Membranes provide an alternative to gas separations, but are not always necessarily advantageous over other existing processes. There are some trade-offs (MacLean, 1986) inherent in membrane process: a membrane with high permeability usually has low selectivity or vice versa. Thus, either a high recovery or a high concentration may

be obtained through a single stage permeation, but seldom both. Also, the choice of operation pressure and pressure ratio affects the power consumption and the capital cost oppositely. Since it is a rate process based on the difference in permeation rates of species, and all components will permeate, to some extent, through a membrane, an ideal separation producing one or more ultra-pure streams can not be achieved economically. Baldus and Tillman (1986) give some simple rules that gas separation by membranes is favorable:

1. when moderate purity and recovery are sufficient,
2. when the components to be separated are in considerable amount,
3. when the feed gas is available at the necessary pressure, or
   when the residue stream is needed at high pressure,
4. when the feed gas contains no substances harmful to membrane,
5. when a membrane with sufficient selectivity is available.

In consideration that membrane is especially effective to effect partial separation, the combination of membrane and other suitable conventional techniques such as absorption, adsorption and cryogenic is more economical than a scheme where the full separation is to be effected by either process alone (Beaver et al., 1988; MacLean, 1986).

1.3 About the Thesis

This thesis is involved in gas-gas and gas-vapor separations:

a) The pore flow model proposed by Chen et al. (1989) is extended to describe gas mixture permeation. Experimental data of CH_4/CO_2 permeation through asymmetric cellulose acetate membranes are analyzed and interpreted based on the extended model.

b) Using a phase inversion technique, asymmetric polyimide membranes are prepared for the separation of organic vapors from contaminated air. The effects of membrane making parameters such as membrane casting solution composition, evaporation temperature and evaporation time are investigated.

Chapter 2

Literature review

Many books, reports and review papers provide a substantial amount of information on membrane separation processes. Lonsdale (1982, 1984) gives an interesting look at the growth and evolution of membrane technology, and provides a review of the current development state. The book co-authored by Sourirajan and Matsuura (1985) is full of extensive information about material selection, membrane making, transport fundamental, process design as well as applications. Lloyd (1985) edited a book in which the material sciences of synthetic membrane are reviewed. The phase inversion method for the preparation of membranes is discussed in detail by Kesting (1971). Matsuura and Sourirajan (1988) wrote a textbook on the recent progress in membrane processes. Moreover, Scott (1980) and Torrey (1984) edited the U.S. patent literature regarding membranes during 1978–1980 and 1982–1983 into books which contain much detailed, descriptive technical information usually not available in the journal literatures.

2.1 Requirements for Membranes

The permeation of a gaseous component through a membrane can to a first approximation be described by

$$[PR]_i = \frac{P_i}{l} \Delta p_i A \tag{2.1}$$

where $[PR]_i$ = permeation rate of component i,

P_i = membrane permeability to component i,

Δp_i = partial pressure difference of component i,

A = membrane area,

l = effective thickness of the membrane.

The precise effective thickness of a membrane, in particular an asymmetric membrane, is often unknown. Therefore membrane permeability is frequently expressed in terms of the thickness-normalized permeability, (P_i/l), which can easily be determined from experimental data. Essentially, (P_i/l) is the permeation flux per unit pressure difference across the membrane From an engineering point of view, (P_i/l) is more important than P_i alone. (P_i/l) will be used afterwards to characterize the permeability of a membrane in this study and renamed as J_i.

The separation factor for component i over component j in a mixture is defined by

$$[SF]_{i/j} = (Y_i/Y_j)/(X_i/X_j) \tag{2.2}$$

where X's and Y's are the mole fraction of the components in the feed and the permeate, respectively. $[SF]$ is affected by operating conditions. When the permeate pressure is negligible compared to the feed pressure, the separation factor can be related to the ratio of the permeabilities of components i and j, $\alpha_{i/j}$, which is given

by

$$\alpha_{i/j} = \frac{P_i/l}{P_j/l} = \frac{J_i}{J_j} \tag{2.3}$$

The permeability ratio is a separation index similar to the relative volatility in distillation. It provides a measure of the permselectivity of a membrane. When $\alpha_{i/j} = 1$, no separation occurs. $\alpha_{i/j}$ is usually called ideal separation factor (Chern et al., 1985).

It can be seen from Eqs.(2.1) and (2.3) that for a membrane process to be realistic, the membrane has to satisfy a number of requirements, including (1) high permeability, (2) high selectivity, (3) high membrane area per unit volume, i.e. membrane area density, (4) high stability, i.e. good chemical, mechanical, and thermal properties, and (5) ease of fabrication. The intrinsic permeability and selectivity of a membrane are mostly determined by the membrane material; the membrane area density is controlled by the engineering approach of membrane making, while the stability is affected by both of them. In the field of gas separation by membranes, there is therefore a constant search for membrane materials with favorable properties, and techniques of fabricating a membrane of small effective membrane thickness and large membrane area density.

2.2 Current research

The current research work can be divided arbitrarily into 6 aspects, which contribute toward the same goal — to improve the separation efficiency of membrane technology.

1. Searching for good polymer materials. (e.g. synthesis of new polymers; modification of existing materials such as copolymer, blends, crosslinking, grafting,

additives.)

2. Reducing the effective thickness of membranes. (e.g. asymmetric membranes, composite membranes, ultrathin membranes.)

3. Increasing membrane area density. (e.g. hollow fiber type, spiral wound type and their variants.)

4. Modelling and process design. (e.g. module configuration and arrangement, flow distribution, module size optimization, cascade operation with or without reflux, hybrid processes.)

5. Developing alternative promising approaches. (e.g. continuous membrane column, multi-membrane permeator, carrier-mediated membranes.)

6. Understanding membrane processes. (e.g. permeation mechanism, membrane characterization, structure–performance relationship, effects of operating factors on membrane performance.)

2.3 Screening of Membrane Materials

Polymer materials are utilized overwhelmingly for the gas separation membranes (Sengupta and Sirkar, 1986). High permselectivity and resistance to penetrants and contaminates attack are required for membrane technique to compete with the traditional processes. Membrane material determines the packing density and segment mobility of polymer chains, and consequently affects the interaction between penetrants and a membrane (Lloyd, 1985).

In the past, the membrane materials for gas separation were often selected empirically, rather than on the basis of scientifically formulated principles (Lloyd, 1985). Almost every polymer that can be formed into a membrane has been characterized in terms of gas permeabilities, and the list of polymer membrane materials is virtually endless insofar as possible chemical varieties are concerned. Therefore there is a great deal of data in the literature about the permeation of gases through polymer membranes. Based on this information, Chern et al. (1985) and Strathmann et al. (1986) proposed a possible approach to select the appropriate candidate membrane materials in terms of physicochemical interactions for gas mixture separations. This approach is reasonably effective for screening available polymers, however, does not provide a guideline to improve membrane performance by scientific alteration of polymer structure.

The forces that lead to the physicochemical interactions involved in membrane transport are present in other situations where permeating components and membrane are in contact with one another. Long et al. (1988) used a gas chromatographic method to select membrane materials on the basis of sorption characteristics of gases in a polymer material which was packed in the column. It is expected that this method can offer a simple means of building a data base for membrane material selection.

A great number of studies have been done on the relationship between the chemical structure of polymers and their permeabilities to gases (Cifuentes et al., 1986; Kim et al., 1988). It has been shown that the substitution of some functional groups into the polymer chains or side chains may result in a significant improvement in permeability. This suggests that new polymers with good permselectivities will be able to be tailor-made by scientific alteration of polymer structure. These new polymers

have been added to the list of available membrane material candidates.

The commercial success of gas separation by means of membrane indicates that polysulfone, cellulose acetate, silicone-based polymers and their combination have attained wide application (Finken, 1985). The preparation of these membranes will be briefed in the following section.

Recently, polyimide membranes have been of great interest in developing gas separations at high operation temperature because of their excellent thermal stability and chemical resistance. Now, materials for gas separation membrane have been extended to other polymers such as poly(phenylene oxide) derivatives, poly(4-methyl 1-pentene), and aromatic polyamides because of their good physical and mechanical properties (Haggin, 1988).

In general, the selectivities of polymer membranes for gas permeation vary inversely with their intrinsic permeabilities. Silicone rubber has previously been considered as the most gas-permeable polymer. However, a new polymer, poly(1-trimethylsilyl -1-propyne) (PMSP) has been developed recently which shows a gas permeability (toward O_2, N_2, CO_2, CH_4, and He) of about an order of magnitude higher than that of silicone rubber (Takada et al., 1985). It is particularly interesting that O_2/N_2 selectivity of PMSP is about equal to that of silicone rubber, while CO_2/CH_4 selectivity is higher. The modification of PMSP membranes shows that the instability of permeation properties in the early stage can be overcome, and it seems to be prospective as a membrane material for air separation (Nakagawa et al., 1987). This new material also suggests it be possible to synthesize polymers exhibiting both a high permeability and a high selectivity.

2.4 Membrane Making

Membrane preparation procedure determines the membrane morphology, and accordingly influences the membrane performance and transport property. The most important membranes used today are structurally asymmetric, which can be prepared in two ways, one via phase inversion process, the other by depositing an extremely thin polymer film on a microporous substructure (Strathmann, 1986). The majority of commercial membranes are produced by the so-called phase inversion method.

2.4.1 Phase Inversion Process

According to Kesting (1985), the phase inversion process is a process that homogeneous polymer solution is transformed into a two-phase system in which polymer-rich solid phase forms the rigid membrane structure, while polymer-poor liquid phase forms the voids. To prepare this kind of membrane, the polymer is dissolved in a solvent. The homogeneous solution is formed into a film in such a way that the desired shape (e.g. flat, tubular, or hollow fiber) is obtained. The polymer solution is treated in a specific way to precipitate the polymer, followed by a suitable drying process. Thus the dry membrane for gas separation is obtained.

In the precipitation step, several techniques have been developed to achieve phase inversion (Wijmans and Smolders, 1986):

- Precipitation from vapor phase
- Precipitation by controlled evaporation
- Immersion precipitation

- Thermal precipitation

The immersion precipitation technique, first developed in 1960 by Loeb and Sourirajan for the preparation of revers osmosis membranes, has been applied widely for the production of skinned membranes for various applications. The feature of the technique is that the cast polymer film is either allowed to partially evaporate prior to immersion in a nonsolvent gelation bath, or immersed directly into a nonsolvent bath. Then the polymer precipitates as a result of solvent exchange with nonsolvent. The process, involving solvent–nonsolvent exchange, is also termed as wet process. According to Reuvers and Smolders (1987), the following steps can be used to illustrate the membrane formation process chronologically:

1. After casting, the polymer solution film may be subjected to evaporation, which may induce an asymmetric profile in the film;
2. Upon immersion of the film in a nonsolvent bath, exchange of solvent and nonsolvent takes place, which may result in an asymmetric profile and metastable composition in the film;
3. When metastable composition reaches in the film, demixing process may occur, which is responsible for the porosity of the ultimate membrane.

It has been identified that in this procedure several parameters influence the structure and properties of the membrane (Strathmann, 1986), including:

- The polymer and its concentration in the casting solution,
- The solvent or solvent system,
- The precipitant or precipitant system,

- The precipitation temperature.

- Other parameters involved in the evaporation step and the annealing step.

Strathmann (1985) explored the phase inversion mechanism and the influence of the parameters involved in the procedure for membrane preparation. The membrane formation procedure is rationalized with the aid of a three-component phase diagram. Since phase inversion is actually a nonequilibrium process, kinetic factors are more important. Slow precipitation results in a sponge-like structure, while fast precipitation results in finger-like macrovoids. It is claimed that the scientists of Monsanto Co. (Haggin, 1988) have been able to control the thermodynamic and kinetic parameters of the polymer precipitation so that a new class of asymmetric membranes, whose permeability can be increased significantly without sacrificing selectivity, has been created.

Kesting (1971) discussed in detail the process variables involved in membrane preparation and their effects on the structure of the resulting membranes, including the post treatment and modification. It has been observed that through proper control of process variables, the same membrane structures can be obtained from various polymers and that the same polymer can be used to achieve various membrane structures. In principle, phase inversion membranes in a large variety of structures can be made from almost every polymer, and these membranes can also be tailor-made for a specific separation task (Strathmann, 1986). Therefore, phase inversion technique has been studied intensively and utilized widely.

2.4.2 Cellulosic Membranes

Cellulosic membranes have been used in the past and are still widely used for gas separation, with cellulose acetate and modified cellulose acetates (CA) comprising a major commercial material in this field.

The wet Loeb-Sourirajan type of cellulose acetate membranes can not be directly used for gas separation because they tend to lose their permselective properties due to the sublayer collapse. Different techniques of drying the membrane have been developed:

a) Gantzel and Merten (1970) produced the first dry asymmetric CA membrane by quick freezing and vacuum sublimation at -10^0C;

b) Vos and Burris (1969) developed a simple method to dry CA membrane: soaking the water-wet membrane in an aqueous surfactant solution to reduce the water-polymer interfacial tension, and then drying it in air;

c) Using the same idea of reducing the interfacial tension with solutions, Schell (1982) prepared the dry CA membrane through successive solvent exchange steps followed by air drying;

d) Manos (1978) improved Schell's solvent exchange method by contacting the water-wet membrane with at least one replacement liquid, then removing water by decanting or centrifuging, followed by evaporation to remove the replacement liquids.

A number of companies such as Dow, Separex, Envirogenic and Grace are involved in either hollow fiber or spiral wound modules of CA membranes (Zhu and Liu, 1988). Though little detailed information is available concerning the membrane performance in actual gas separation applications, the unique behavior of cellulose acetate membranes was supported by Koros (1983). It was found that of all the glassy polymer membranes studied, only cellulose acetate membrane showed a favorable

pressure dependence of permeability to CO_2. The CO_2 permeability monotonically increased by 138% if pressure changes from zero to 20atm (2026kPa). Though cellulose acetates may be somewhat less tolerant to a high temperature, they are so effective first-generation membrane materials that they have served as one of the standard materials for the development of novel separative polymers (Finken, 1985).

2.4.3 Non–Cellulosic Membranes

Ward and coworkers (1976) pioneered the use of block copolymer to combine the high permeability of rubbery polymers and the high selective function of glassy polymers. To reduce the membrane thickness, they used the Langmuir–Blodgett technique in preparing the membranes.

Henis and Tripodi (1980a,b, 1981) of Monsanto Co. used high strength, high selective polysulfone as membrane material. Since it is difficult to get the defect–free skin–layer of an asymmetric glassy polymeric membrane, a thin, non–selective, high permeable polymer such as silicone rubber film is coated to plug the defects in the skinned polysulfone membrane against a high flow rate of unseparated gases. Thus, high separation is obtained in this kind of membrane which is, generally speaking, an asymmetric, composite membrane. It is not necessary for the coating polymer itself to be highly separative to gas mixtures as long as it is highly permeable as not to significantly reduce the permeabilities of gases through the composite membrane. But it should be impermeable enough to act as a barrier to the flow of unseparated gases. This type of membrane was entitled as resistance model membrane by its inventors, though some researchers prefer the term coated integrally–skinned composite. In addition to polysulfone(A) – silicone rubber(B) composite membrane, a number of other composite membranes of this type have been studied, for instance, polysulfone(A)

– polyethylene(B), polyacrylonitrile(A) – silicone rubber(B), polyacrylonitrile(A) – polyethylene(B) and polyetherimide(A) – silicone rubber(B), where A designates the skin and B designates the coating (Stern, 1986).

In stead of coating, a lamination method was proposed. According to Chen (1989) who studied silicone rubber laminated polysulfone membranes, the laminating film functions similarly to the above coating approach, but the mechanism is a little different. The lamination approach is very effective in mechanism study since the thickness of the laminating layer is much easier to determine than that of a coating layer. However, the preparation of membrane laminates is a delicate operation because the two layers should be closely contacted. Otherwise any space between the two layers may cause a significant loss of the membrane performance.

A promising alternative approach to composite membrane is the reverse of Monsanto's leak–stopping technique. In this attractive case membrane support is highly porous, and a thin selective coating (about 1000 to 2500Å thick) is formed on the top of the porous support by means of interfacial polymerization (Conover, 1986). The coating layer, which can be formed from a wide range of monomers, is responsible for the separation, while the highly porous substrate acts only as a support. Such membranes are known as thin– or ultrathin–film composites, or unintegrally–skinned composites in order to distinguish from skinned membrane composites. For this type of composite membrane that consists of a skinless porous substrate and a dense layer, permeability and selectivity may be solely determined by the permeation resistance of the dense layer. Different polymers may be used as the barrier layer and the porous support, which permits a combination of properties that are not available in a single material. Though this approach has been the basis of reverse osmosis membranes commercialized by Film Tech and UOP, it has not been launched to market for gas

separation because of the problem that swelling stresses might dislodge the coating layer. Nevertheless it is likely to see more emphasis in the future.

Van der Scheer and Werner (1987) patented a technique for the preparation of a three–layer membrane composite by means of plasma polymerization for the production of the selective ultrathin top layer. The membrane comprises (a) a porous support (low pressure side), (b) a highly permeable, not necessarily selective, intermediate layer (e.g. silicone rubber) and (c) an ultrathin selective top layer (high pressure side). If the intermediate layer is not used, the top layer must have sufficient mechanical strength to bridge the pores of the support layer at large pressure difference. It is the intermediate layer that provides mechanical stability without increasing much permeation resistance so that the selective top layer can be ultrathin without any mechanical strength requirement.

2.5 Transport Mechanism

A proper understanding of the membrane separation mechanism may provide with directive information on the research and development of an appropriate membrane. It is essential to specify membrane and membrane systems, interpret the available performance data from laboratory and pilot plants, and predict the membrane performance under given conditions, which are fundamental to engineering design and operation. Because of the complicated penetrants–membrane interactions it is difficult to formulate a single explanation to the complex transport process.

There are several approaches towards understanding of vapor and gas transport through membranes. It seems that most of the approaches can be categorized on the basis of considering the membrane as porous or nonporous. From the mechanismic

point of view, the free volume model (Stern, 1976) and the dual sorption model (Vieth et al., 1976) are very effective in the analysis of sorption, unsteady- and steady-state permeation through the so-called nonporous membranes.

Recognizing that the permeation process is governed by both the chemical nature of the membrane material and the physical structure of the membrane, the surface force – pore flow model (Agrawal and Sourirajan, 1970) takes into account the porous structure of membranes and the phsicochemical properties of penetrant molecules, and offers detailed information of the transport process on a molecular basis. This model can be used to characterize a membrane and predict its performance for the permeation of any gas from the reference gas permeation data (Rangarajan et al., 1984). Moreover, the basic idea of pore flow model has been successfully applied to reverse osmosis, ultrafiltration and, more recently, pervaporation separation (Matsuura and Sourirajan, 1989; Sourirajan, 1989).

2.5.1 Surface Force – Pore Flow Model

This model assumes the presence of pores in the surface layer of an asymmetric membrane, which are equivalent to capillary tubes. The diameter of such a pore may be any distance, however small, greater than zero. Also assumed is that there exists an equilibrium adsorption of gas molecules on the wall of pores, and the adsorbed gas molecules are mobile. Thus the surface flow takes place under a concentration gradient, and contributes to the overall permeation.

For an individual pore, in addition to the surface flow, one of the three mechanisms, namely, (1) Knudsen flow, (2) slip flow, and (3) viscous flow may occur, depending on the ratio of the pore radius r and the mean free path of gas molecules

λ. Knudsen flow occurs in the range of (r/λ) between 0 and 0.05; slip flow occurs in the range of $(r/\lambda) = 0.05$ to 50; viscous flow occurs when (r/λ) is greater than 50.

In the case of a membrane with a distribution of the pore size, all the four mechanisms may occur simultaneously, depending on the operation conditions. Therefore the total transport of gas is given by summing up the transport of gas through each pore, applying the relevant flow mechanism. Assuming a normal distribution of the pore size on the membrane surface, Rangarajan et al. (1984) derived a mathematical expression of the total flux of gas permeation. However, when it is used to fit experimental data, negative values of the average pore size sometimes occur. To prevent this unreasonability, Fouda et al. (1987) use a normal pore size distribution in logarithmic scale in their derivation of transport equations, which appear to be fairly good to describe the permeation process through an asymmetric membrane.

Assuming a uniform pore size distribution on the membrane surface and the monolayer adsorption of gases on the wall of pores, Chen et al. (1989) developed recently a similar model for the permeation of pure gases through asymmetric cellulose acetate membranes. The concept of surface viscosity was introduced to describe the surface flow based on Gilliland's work with some modification. Consider a thin film (thickness t) of adsorbed gas molecules on the surface of a cylindrical pore (radius r) moving in the axial direction at an average velocity u, whose velocity gradient is $(2u/t)$ if a linear velocity profile occurs in the direction vertical to the movement of the film (see Figure 2.1(b)). The shear stress and spreading pressure working on the film must be balanced when a steady state movement of the film is reached, which requires

$$-\mu\frac{2u}{t}\,dx = d\phi \tag{2.4}$$

Starting with this equation the mass flow rate of gas through one pore by surface

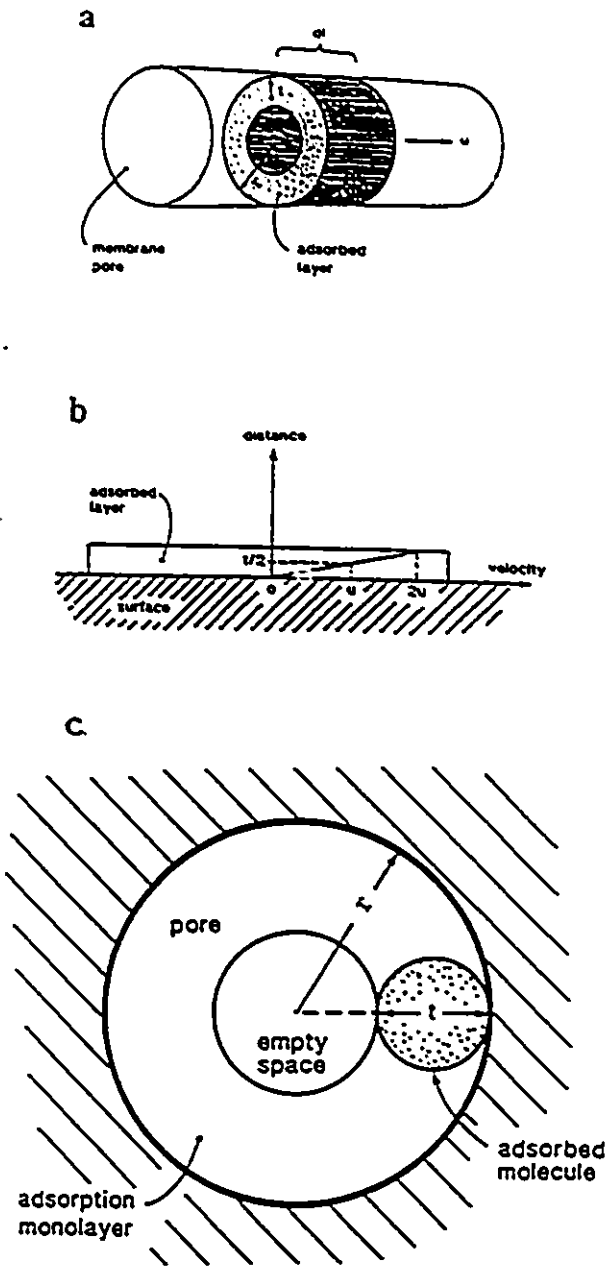

Figure 2.1: Schematic representation of adsorbed monolayer moving in a cylindrical pore.

flow mechanism was derived as

$$q_s = \frac{\pi t^3(2r-t)^2}{8r}\frac{RT}{\mu}k_H^2\frac{\Delta(p^2)}{l} \tag{2.5}$$

The derivation is briefly presented in Appendix A.

Surface flow is usually considered as an anomalous flow that deviates from the expected free molecular flow. It appears to be related to the adsorption of gases on the surface of porous materials. Since the adsorption changes the size of its flow channel, the measurement is quite complicated. For this reason, surface flow has not been well described except in a few particularly simple cases (Fain, 1988). The approach of Chen et al. in which surface viscosity was proposed analogously to the viscosity of fluid flow, provides a easier way of understanding surface flow. Because of the presence of adsorbed gas layer (thickness t) in the pores of radius r, only the circular area with radius being $(r-t)$ permits Knudsen, slip or viscous flow to take place (see Figure 2.1(c)). Similarly, summing up all the transport in each pore gives the total transport, whose expressions are summarized as follows,

$$Q_t = \begin{cases} Q_S & \text{when } t < r \le 1.5t \\ Q_S + Q_K & \text{when } 1.5t < r \le 0.05\lambda \\ Q_S + Q_{Slip} & \text{when } 0.05\lambda < r \le 50\lambda \\ Q_S + Q_V & \text{when } r > 50\lambda \end{cases} \tag{2.6}$$

where Q's are the permeation fluxes in different mechanisms; λ is the mean free path of gas molecules:

$$Q_S = \frac{N_t}{l}\frac{\pi t^3(2r-t)^2}{8r}\frac{RT}{\mu}k_H^2\Delta(p^2) \tag{2.7}$$

$$Q_K = \frac{N_t}{l}\left(\frac{32\pi}{9MRT}\right)^{1/2}(r-t)^3\Delta p \tag{2.8}$$

$$Q_{Slip} = \frac{N_t}{l}\frac{\pi(r-t)^3}{M\bar{c}}\Delta p \tag{2.9}$$

$$Q_V = \frac{N_t}{l}\frac{\pi(r-t)^4}{8\eta RT} p_m \Delta p \tag{2.10}$$

$$\lambda = \frac{RT}{\sqrt{2}\pi d^2 N p_m} \tag{2.11}$$

Surface flow always exists if the monolayer can be formed on the pore surface, which requires $r \geq t$. However Knudsen, slip and viscous flow may or may not occur, depending on the pore size and the mean free path of gas molecules under the permeation conditions.

2.5.2 Other Models

Solution–Diffusion Model. It is assumed that gas molecules dissolve in membrane on the high pressure side, then diffuse through the membrane under a concentration gradient to the low pressure side where they desorb into the gas phase. This mechanism, regarding the membrane as a homogeneous solvent, applies mainly to the defect-free, dense, rubbery membranes but not to the integrally-skinned or thin film composite type of membranes because membrane structures are not considered.

Dual Mode Sorption and Diffusion (Vieth et al., 1976). This mechanism divides gas molecules adsorbed in a glassy polymer into two distinct populations: one is dissolved in the bulk of glassy polymer according to Henry's law, the other is adsorbed in the microvoids of polymer matrix obeying the Langmuir isotherm. The two populations of gas molecules diffuse through the membrane at different mobilities. Many experimental studies appear to have confirmed its applicability to simple gas permeation through glassy polymeric membranes, but it has been argued that carbon–13 rotating–frame relaxation rate measurement indicates only a single population of gas molecules in a gas/glassy polymer system (Raucher and Sefcik, 1983).

Free Volume Model (Stern, 1976). The model basically assumes that the transport rates of components of a mixture in a polymer depend on the free volume of the system, and that the effect of components on the free volume is additive. To predict the permeation flux requires the knowledge of free volume parameters.

Irreversible Thermodynamics (Krishna, 1986). The irreversible thermodynamics theory, in particular the generalized Maxwell-Stefan relations are used to describe the relative motion of species in a mixture. This model gives consideration to various driving forces which may result in relative motion of components across a membrane, and provides relationships between the driving forces and the mass transfer velocities of species. However, this approach does not take the physicochemical properties of gas/membrane system into account.

Several investigators have described the applicability and limitations of the models now in use. The development of the models has been reviewed by Matson et al. (1983).

2.6 Membrane Modules

Essentially, there are four basic configurations (plus numerous variants within each) which have been proposed and developed: hollow fiber, tubular, spiral wound and flat. All of them have strong and weak points. For technical and economic reasons, hollow fiber and spiral wound elements dominate the major plant business for gas separation because they have successfully provided with the most viable approaches of incorporating a large amount of membrane area into a compact module volume to increase the membrane area density, which is a crucial parameter in determining the ultimate size of a gas separation system. It is the coupling of high membrane area

density resulting from these approaches with the low permeation resistance resulting from the asymmetric membrane approach that produces fluxes of several orders of magnitude higher than those of the early membranes in the 1960s (Stern, 1986).

Flat configuration is one of the oldest used historically. It is very popular for simplicity in studying membrane performance and a variety of applications. Flat-plate designs provide a very useful and simple tool in developmental work and laboratory research though they are impractical for industrial applications because of low membrane packing density.

In module design, a number of factors affect the separation performance, such as the pressure drop due to the gas flow on both sides of a membrane, concentration polarization near the membrane surface, and the gas flow distribution along the membrane. They are sometimes related to each other. Consideration of only the transport process inside the membrane will, in general, leads to oversiplification of the membrane process since the overall separation efficiency is influenced by all the imperfections of a module.

A well designed membrane separator should have a uniform velocity distribution of gas flow over the entire membrane surface, but this ideal is impractical because the feed entrance and product exit will always introduce stagnation points and obstructions to flow, which will influence the local velocities. More uniform velocities may be obtained at higher pressure drops, but the available pressure difference across the membrane, i.e. the driving force, is sacrificed. A computation on the module performance shows that the extent of separation and the membrane area required depend on flow patterns. The perfect mixing is the least efficient, whereas the countercurrent flow requires the smallest membrane area (Stern, 1986).

Concentration polarization is a common phenomenon in membrane separation

processes. In the case of gas mixture permeation, the slow component will be retained to some extent. Therefore, a concentration gradient is built up near the membrane surface. As a result, the concentration of the fast gas is lower on membrane surface than that in the bulk gas phase, while the opposite is true for the slow gas. Concentration polarization results in a lower flux and a less extent of separation. In many existing membrane gas separation processes, the effect of concentration polarization is not significant. However, the effect may become predominant for highly permeable and highly selective membranes.

In the case of hollow fiber membranes, higher membrane area densities can be achieved by using smaller diameter fibers and higher packing densities. However, the former will cause a higher pressure buildup in the bore, while the latter will cause a higher pressure loss in the shell side (In most cases feed outside and permeate inside scheme is used). These two together result in a loss of the driving force. This problem can, to some extent, be minimized by optimizing hollow fiber size and packing density, and by arranging the exit and entrance of streams properly. This consideration has obviously been used by Dow Co. in their Generon system design where short length of hollow fiber is used, and feed is introduced through a centrally located distribution tube, while permeate is removed from both ends of the bores. This design allows one to use smaller diameter fibers without serious pressure drop problem.

2.7 Innovative Concepts

The research and development aimed at exploiting membrane technology for gas separation are conducted actively. Attempts have been made to (1) enhance separation extent by using the membrane currently available and (2) develop novel membrane

processes of better performance.

Continuous Membrane Column (Hwang and Thorman, 1980). It consists of an enriching section and a stripping section which function similarly to those in a distillation column. This is an ingenious way of improving separation efficiency of a membrane without any alteration of membrane properties. In principle, it is possible to separate a binary mixture to any desired extent at the operating condition of sufficiently high recycle fraction and low stage cut.

Two–Membrane Permeator (Perrin and Stern, 1985; Sirkar, 1980). The basis of the process is the simultaneous use of two different types of membranes which are chosen to be selective toward different components of the mixture to be separated. The feed is separated into three streams: both of the permeate are enriched in different species, while the residue stream will be enriched in the slowest component if ternary gas mixture is to be separated.

Permeators With Sweeping Stream (Pan and Habgood, 1978a). Sweeping a stream of gas on the permeate side will decrease partial pressure of the permeated components, accordingly increase their driving force for permeation. With suitable sweeping agent and proper amount of sweeping, the membrane area requirement can be reduced while the permeate stream is insignificantly diluted.

Facilitated Transport Membrane (Gottschlich et al., 1988). This new approach uses a specific carrier incorporated within the membrane to improve the permselectivity. In some cases carrier reacts with target species reversibly and shuttles forth and back across the membrane so that the transport is facilitated.

Plasma Polymerized Membrane (Lonsdale, 1984). This kind of membrane is produced by depositing a polymer, which is formed in the vapor state from a monomer gas, onto a suitable substrate. The properties of plasma polymers are quite

different from those polymers by free radical polymerization. Plasma polymerization opens new possibilities to prepare and modify membranes, however, the problem of reproductivity in membrane properties has not been solved yet.

Chapter 3

Data Analysis of CO_2/CH_4 Mixture Permeation Through Cellulose Acetate Membranes

Cellulose acetate membranes have been commercially applied to gas separation because of their good properties and commercial availabilities. Since the cellulose acetate membranes for reverse osmosis are generally produced in a water-wet condition, in order for such a membrane to be useful for gas separation, it is necessary to dry the membrane without damaging its structure because the membrane structure governs the separation properties.

Solvent exchange method is one of the techniques of removing the water within membranes. Chen et al. (1989) studied the permeation of He, CO_2 and CH_4 through this type of membranes, and established transport equations for pure gas permeation on the basis of the surface force – pore flow mechanism. In this thesis the transport equations are to be extended to analyze gas mixture permeation data. The

experiments were performed by Chen[1] at the National Research Council of Canada, Ottawa. All the experimental data analyzed in the work were provided by Chen and given in Appendix B.

3.1 Experimental

Membrane preparation. Membranes were cast on glass plates at 30°C, and at 65% relative humidity from a casting solution whose composition was (wt%): cellulose acetate 17, acetone 69.2, magnesium perchlorate 1.45, and water 12.35. After 60 seconds of evaporation, the membranes were gelled in ice cold water and then heat-treated using hot water at temperatures ranging from 60°C to 80°C. To dry the membrane multiple solvent exchange technique was used. The water in the membrane was successively replaced by solutions of the first solvent and water. In the latter solvent replacement process, the solutions of progressively higher concentrations in the first solvent were used. The first solvent was then replaced by a volatile second solvent which was subsequently air evaporated to obtain the dry membranes. In this study ethanol or isopropanol was used as the first solvent, and hexane as the second solvent.

Membrane testing. Carbon dioxide and methane mixtures were used as feed gases, in which the mole fraction of carbon dioxide varied from 0.1 to 0.9. The permeate side was kept at atmospheric pressure, while the feed pressure was in the range of 50psig (446kPa abs.) to 300psig (2168kPa abs.). The experiments were performed at room temperature. The permeation fluxes of individual components

[1]Present address: Dalian Institute of Chemical Physics, Chinese Academy of Sciences, 129th Street, Dalian, China.

were determined by the overall permeation rate, measured by a bubble flow meter, and the permeate composition measured by a gas chromatograph.

3.2 Data Analysis

According to Chen et al., the radius of a cylindrical channel for porous flow, $(r-t)$, is less than 0.05λ for both carbon dioxide and methane for all the membranes over the entire pressure range under study. This suggests that the gas permeation is controlled by both Knudsen flow and surface flow, or surface flow alone, depending on the pore size of the membrane.

In the analysis of pure CO_2 and CH_4 permeation through the membranes, the following assumptions have been made (Chen et al., 1989):

- CO_2 molecules are cylindrical when they are adsorbed on the surface of a pore. They lie on the surface with their axes parallel to the axis of cylindrical pore channel, and form a monolayer. The thickness of the monolayer, t, is equal to the diameter of the cylindrical molecule, which is 3.3×10^{-10}m.

- Though CH_4 molecules are tetrahedral, they are considered as spheres. The thickness of the adsorbed molecule monolayer, t, is equal to the diameter of the sphere, which is 3.84×10^{-10}m.

- The concentration of gas molecules in the adsorbed monolayer is in equilibrium with the pressure of the gas phase, and the monolayer adsorption can be described by Henry's law. The Henry's constant, k_H, has been calculated to be 1.972×10^{-2} and 2.316×10^{-3} mol/m^3.Pa respectively for the adsorption of CO_2 and CH_4 on cellulose acetate material.

- Helium adsorption on polymer materials is negligible. Therefore, helium permeation through the membranes is controlled by Knudsen flow mechanism alone.

In practice, it is impossible to know the number of pores per unit membrane area, N_t, and the effective thickness of the membrane, l. However, the ratio (N_t/l) for a reference membrane (membrane of the smallest pore size) could be calculated from the data of helium permeation as 3.68×10^{19} m^{-3}. It was further assumed that (N_t/l) was identical for all the membranes under study. Using this value, the average pore size on the membrane surface was obtained. The pore radius so calculated for all the membranes under study was in the ranges of 3.84×10^{-10}m to 11.69×10^{-10}m. Literature [9] (Chen et al., 1989) has to be referred for more detailed information.

To describe gas mixture permeation through the membrane, the following assumptions are made:

- Monolayer adsorption remains valid for the adsorption of the gas mixture.
- The thickness of the adsorbed gas layer is equal to the diameter of the larger molecules when a binary gas mixture system is considered.
- The concentration of a component in the adsorption monolayer is proportional to its partial pressure in the gas phase, and the proportionality constant is independent of the presence of the other component.
- Surface viscosity is affected by the interaction between gas molecules in the adsorbed layer.

Following Eqs.(2.7) and (2.8), and on the basis of the above assumptions, the total permeation flux of a component in a gas mixture by surface flow and Knudsen

flow can be written as

$$Q_{t,i} = \frac{N_t}{l}[\frac{\pi t^3(2r-t)^2}{8r}\frac{RT}{\mu_i}k_{H,i}^2(p_{h,i}^2 - p_{l,i}^2) + (\frac{32\pi}{9M_iRT})^{1/2}(r-t)^3(p_{h,i} - p_{l,i})] \quad (3.1)$$

where $p_{h,i}$ and $p_{l,i}$ are the partial pressure of component i on feed side and permeate side, respectively.

By definition the permeability can be expressed as

$$J_i = \frac{Q_{t,i}}{\Delta p_i} = \frac{N_t}{l}[\frac{\pi t^3(2r-t)^2}{4r}\frac{RT}{\mu_i}k_{H,i}^2 p_{m,i} + (\frac{32\pi}{9M_iRT})^{1/2}(r-t)^3] \quad (3.2)$$

where $\Delta p_i = p_{h,i} - p_{l,i}$, is the difference in the partial pressure of component i across the membrane; $p_{m,i} = (p_{h,i} + p_{l,i})/2$, the average partial pressure of component i within the membrane.

For the case where the pore size is sufficiently small so that Knudsen flow can be neglected, Eqs.(3.1) and (3.2) will be reduced to Eqs.(3.3) and (3.4), respectively.

$$Q_{t,i} = \frac{N_t}{l}\frac{\pi t^3(2r-t)^2}{8r}\frac{RT}{\mu_i}k_{H,i}^2(p_{h,i}^2 - p_{l,i}^2) \quad (3.3)$$

$$J_i = \frac{Q_{t,i}}{\Delta p_i} = \frac{N_t}{l}\frac{\pi t^3(2r-t)^2}{4r}\frac{RT}{\mu_i}k_{H,i}^2 p_{m,i} \quad (3.4)$$

The following steps are used to test the validity of the above expressions:

1. Calculate the surface viscosity for each component and for different membranes at different operating pressures and compositions;

2. Correlate surface viscosity with the pore size of the membrane and the average partial pressure of the component concerned within the membrane;

3. Compare experimental values of permeation flux with those calculated by Eq.(3.1) or Eq.(3.3) as the case may be, using correlations obtained in step 2;

4. If they are in agreement, predict membrane performance and interpret permeation behavior.

The analytical results are presented afterwards.

3.2.1 Correlation of surface viscosity

The average pore radii on the membrane surface were calculated as 3.84, 4.77, 4.92, 7.76, 8.87, 10.56, and 11.69Å for the seven membranes under study (Chen et al., 1989). For a given membrane, all numerical values of the parameters in Eq.(3.1) or Eq.(3.3) are known except the surface viscosity. From CO_2/CH_4 gas mixture permeation data, surface viscosities were calculated for all the membranes having different pore sizes as functions of average partial pressures. Figure 3.1 represents the results of the membrane with a pore radius of 7.76×10^{-10}m. For other membranes of different pore sizes similar results were generated. The figure shows that the surface viscosity increases rapidly with an increase in average partial pressure, p_m, when it is low, and levels off at high p_m values.

Considering $\log \mu$ versus p_m plots, an asymptotic equation

$$\ln \mu = \frac{k p_m}{1 - K p_m} \tag{3.5}$$

can be used as an empirical expression to characterize the surface viscosity. The coefficients k and K in Eq.(3.5) can be determined using the least–square technique. Rearrangement of Eq.(3.5) yields

$$-\frac{1}{\ln \mu} = -\frac{1}{k p_m} + \frac{K}{k} \tag{3.6}$$

Eq.(3.6) suggests a linear relationship between $1/\ln \mu$ and $1/p_m$. Figure 3.2 shows that Eq.(3.5) is a fair approximation to represent the surface viscosity data given

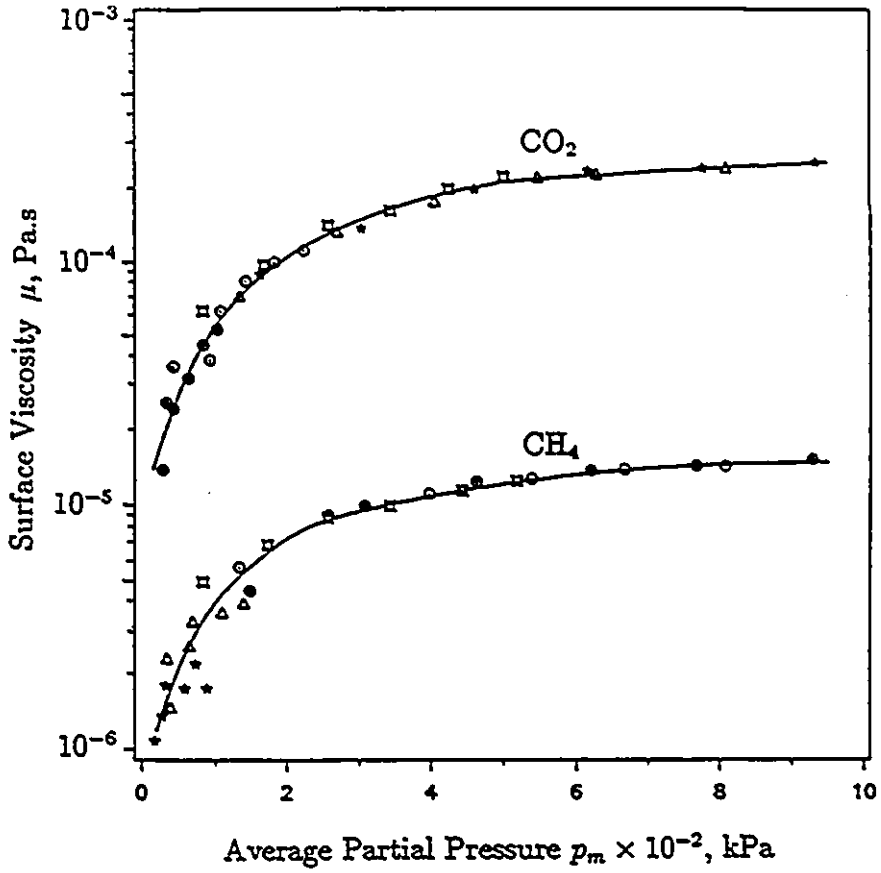

Figure 3.1: Surface viscosity as a function of the average partial pressure. $(\oplus)$,$X_{CO_2} = 0.1016$, $(\odot)$,$X_{CO_2} = 0.2180$, $(\square)$,$X_{CO_2} = 0.5010$, $(\triangle)$,$X_{CO_2} = 0.7870$, $(*)$,$X_{CO_2} = 0.8998$. $r = 7.76 \times 10^{-10}$m.

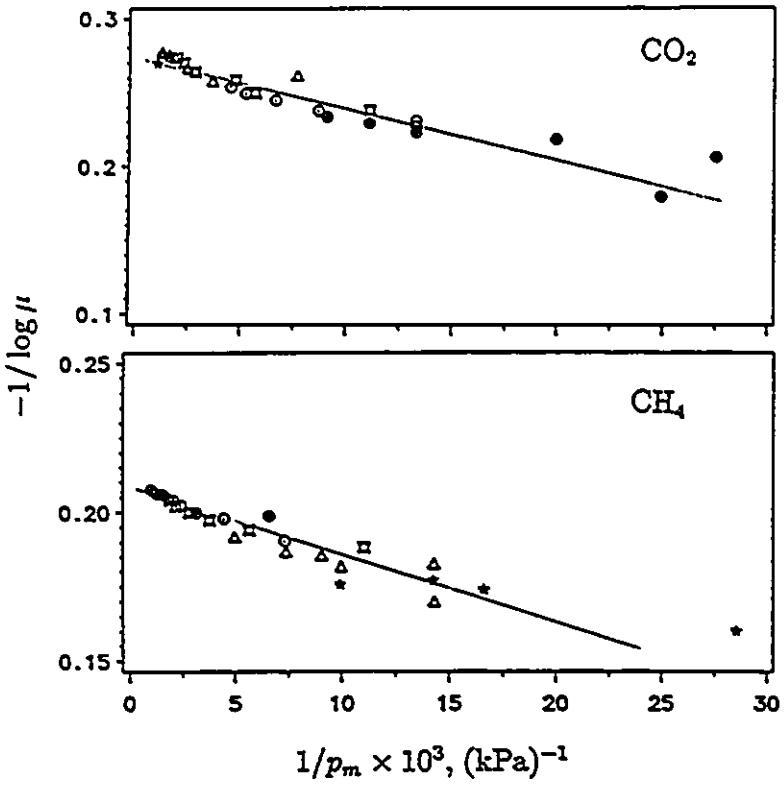

Figure 3.2: Linear relationship between $1/\log\mu$ and $1/p_m$. $r = 7.76 \times 10^{-10}$m. Different symbols correspond to different feed concentrations, and they are the same as those given in Figure 3.1.

in Figure 3.1. Correlation coefficients above 0.98 were obtained for both methane and carbon dioxide. According to Eq.(3.6), $-\frac{1}{k}$ and $\frac{K}{k}$ are obtained from the slope and the intercept of the $-\frac{1}{\ln \mu}$ versus $\frac{1}{p_m}$ plot. Figure 3.3 shows the k and K data as a function of ψ for different membranes, where $\psi(= d/2r)$ is an indication of the relative magnitude of the gas molecule size with respect to the pore size.

Surface viscosity increases when the average partial pressure increases. This means that increasing the packing density of adsorbed gas molecules in the pore produces a higher viscosity. In view of the fact that for polymeric membranes gas permeation can take place to some extent, however small the fluxes may be, and that the membranes having 100% rejection have never been achieved, there are always some pores on membranes which are larger than gas molecules. Gas molecules can not be adsorbed on a polymer so strongly that they stay there for ever. Therefore, surface viscosity can never be an infinite value. From Eq.(3.5) it can be seen that when the pressure is so high that $Kp_m \gg 1$, surface viscosity approaches a limiting value

$$\mu_\infty = \exp(-k/K) \tag{3.7}$$

When pressure is higher than that required for the closest packing of adsorbed gas molecules on the surface of pores, the assumption of monolayer adsorption is no longer valid. In this case the limiting value of the surface viscosity given by Eq.(3.7) is not necessarily true.

Using the data presented in Figure 3.3, surface viscosities of both CO_2 and CH_4 can be calculated from Eq.(3.5) if the pore size on the membrane surface and the average partial pressure within the membrane are known. Figure 3.4 shows the viscosity data at $p_{m,CO_2} = p_{m,CH_4} = 400$kPa as a function of ψ. The surface viscosity of CO_2 is greater than that of CH_4. In the range of small ψ values, CO_2 viscosity

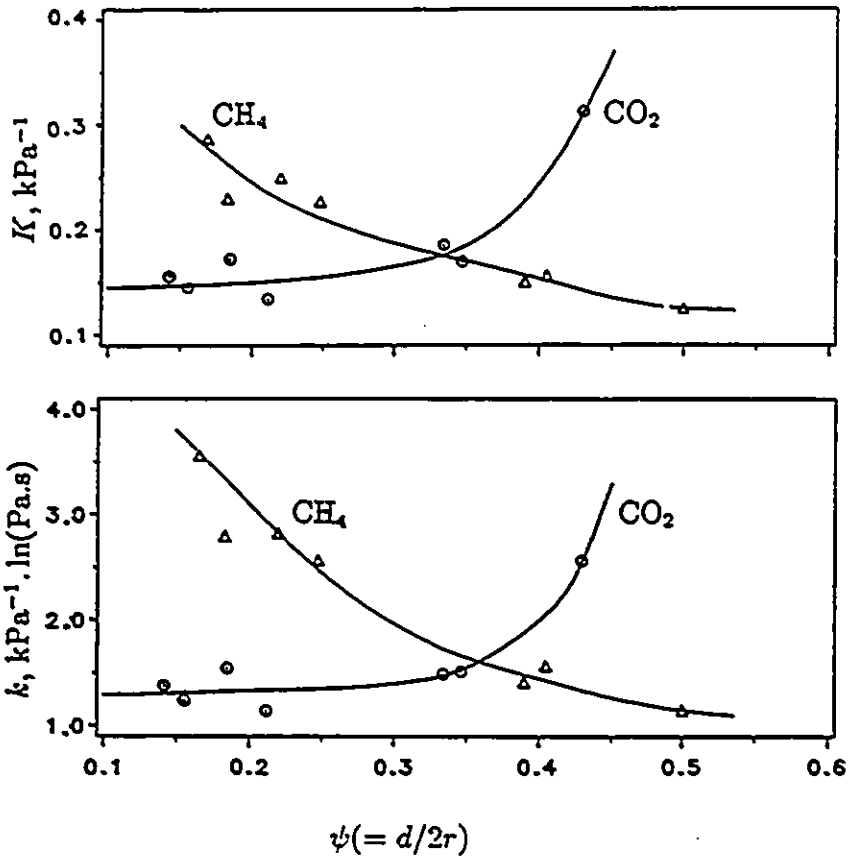

Figure 3.3: Plots of K and k versus ψ. K and κ are constants defined in Eq.(3.3). ψ is the ratio of collision diameter of gas molecules to the diameter of pore on the membrane.

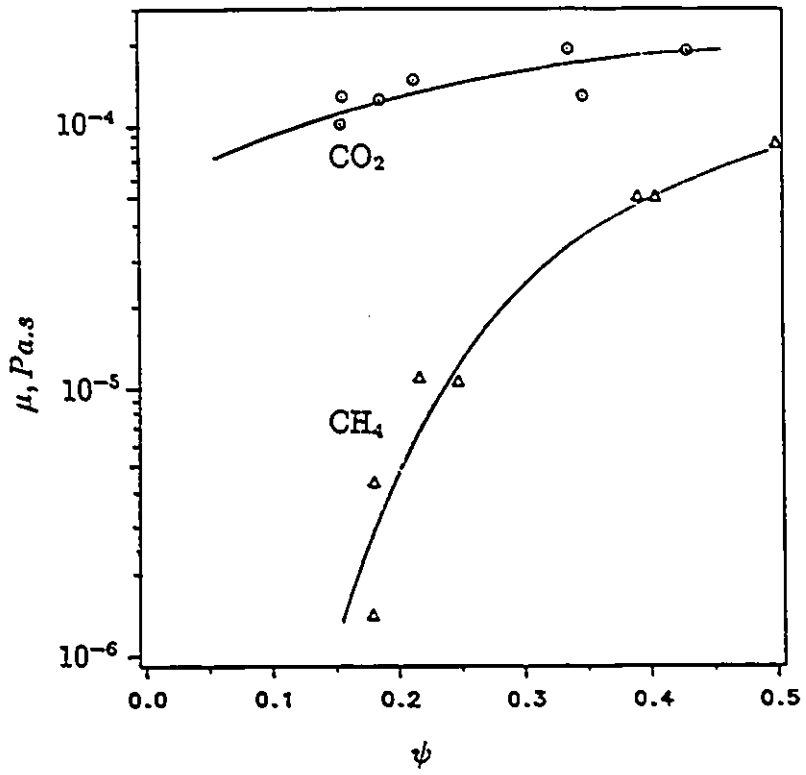

Figure 3.4: Surface viscosity as a function of ψ. $p_{m,CO_2} = p_{m,CH_4} =$ 400kPa.

is nearly one to two orders of magnitude higher than the methane viscosity, which reflects that carbon dioxide molecules have stronger interaction with the polymer surface than methane molecules do. This point is supported by the experiment in which the interaction between gas molecules and polymer materials was investigated (Long et al., 1988).

The surface viscosity increases with an increase in ψ or a decrease in the pore radius r. When the pore size is small, the friction against the movement of gas molecules along the pore is high, resulting in a high surface viscosity. Because carbon dioxide molecules have a smaller size and a higher affinity to cellulose acetate than methane molecules, more CO_2 molecules than methane molecules are accommodated in the pore of the same size under the same operating pressure. As a result the surface viscosity of methane changes rapidly as the pore size changes, while CO_2 surface viscosity undergoes a slight change. These results are in agreement with those observations obtained for pure gas permeation (Chen et al., 1989).

3.2.2 Comparison of experimental data and model calculations

Using the data represented by solid lines in Figure 3.2, the fluxes of individual components can be calculated using Eq.(3.1) or Eq.(3.3) as the case may be under the given operating conditions. Though the data analysis is based on seven membranes with different pore radii ranging from 3.84×10^{-10}m to 11.69×10^{-10}m, only three membranes, which have large, middle and small pore sizes, respectively, are chosen to present the comparison results to see whether the results of the model calculation are in agreement with experimental data. In gas mixture permeation experiments, the

composition and the pressure of the feed gas are two variables which change in the range of 0.1 to 0.9 (CO_2 mole fraction) and 30psig (446kPa abs.) to 300psig (2168kPa abs.), respectively. The comparison is made for different feed pressures at a feed concentration of about 0.5 (CO_2 mole fraction), and for different feed compositions under a feed pressure of 200psig (1479kPa abs.), as shown in Figure 3.5, 3.6 and 3.7. It is clear that the model calculation results are in agreement with the experimental data over the range of experimental conditions. However, the permeation rates calculated by the model are slightly higher than the experimental data in the low feed pressure range, while the opposite is often true when the feed pressure is high. The reason for the deviation may be due to the adsorption hysteresis or the plasticization of the membrane. It has been reported (Chen et al., 1989) that permeation rates are influenced by the sequence of the change in the operating pressure. The permeation rates measured in an experiment starting from a lower operating pressure and ending at a higher operating pressure, which is called the pressure increasing experiment, are slightly different from those obtained in the pressure decreasing experiment, reflecting a pressure hysteresis of the permeation rate. Although the model is far from perfect, it provides with an approach of predicting membrane performance for gas permeation on a molecular basis with an acceptable accuracy.

3.3 Prediction of membrane performance

The permeabilities of CO_2, CH_4 and the separation factor expressed as the permeability ratio can be predicted using the model developed in the preceding section, provided average pore size of the membrane is known. Since the permeability of a component is related to its average partial pressure across the membrane, while its

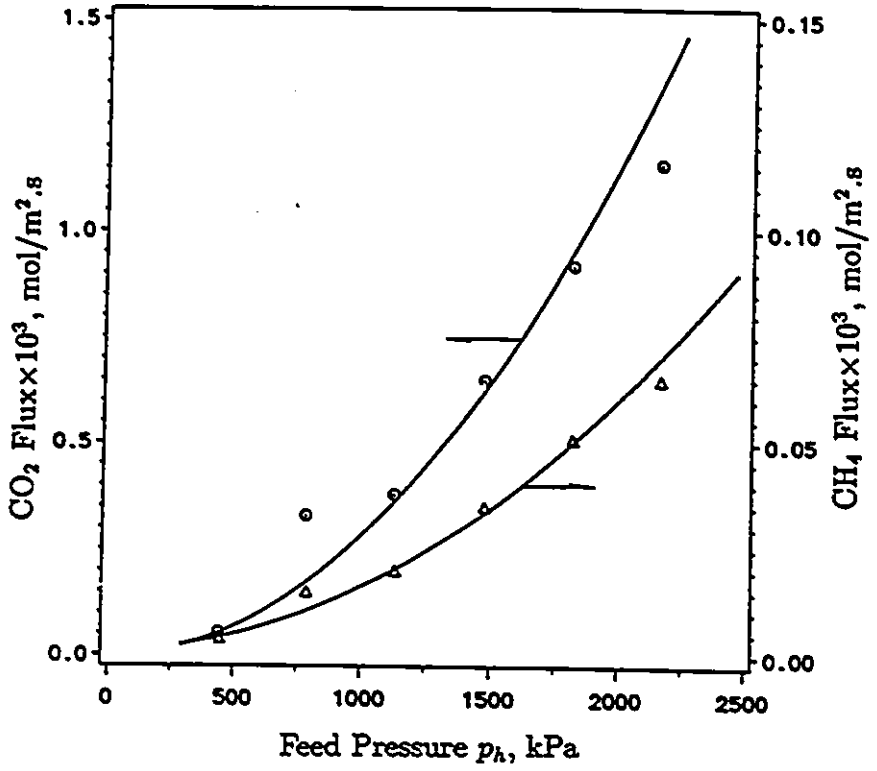

Figure 3.5(a): Effect of feed pressure on gas permeation through the CA membrane for which $r = 4.92 \times 10^{-10}$m. ($\odot$, Δ), experimental data; (———), calculated data. $X_{CO_2} = 0.569$, $p_l = 101.3$kPa.

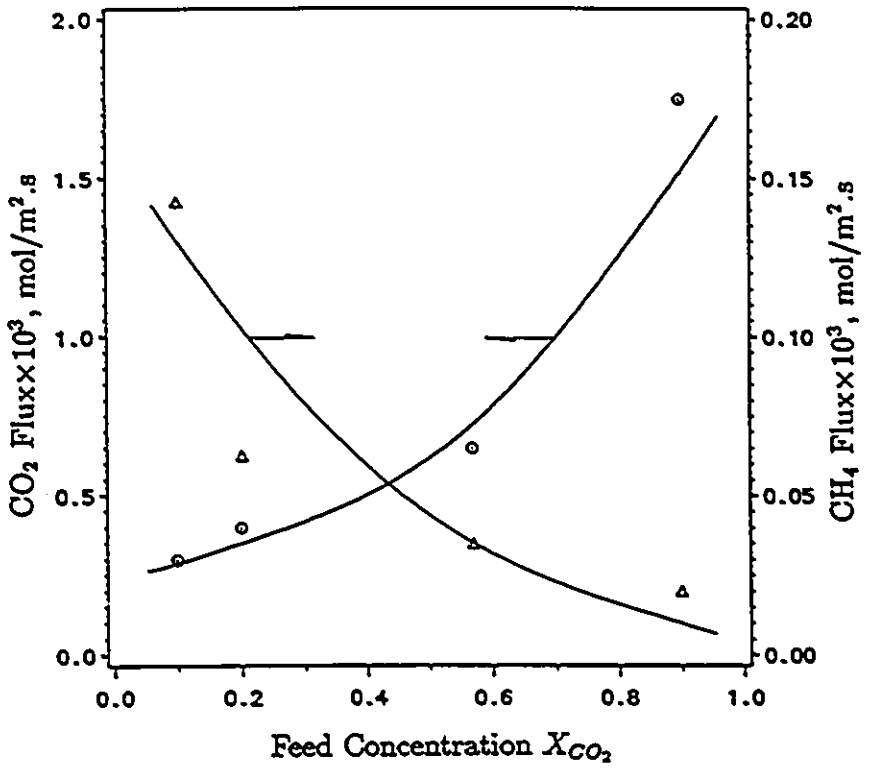

Figure 3.5(b): Effect of feed concentration on gas permeation through the CA membrane for which $r = 4.92 \times 10^{-10}$m. ($\odot$, $\triangle$), experimental data; (———), calculated data. $p_h = 1479$kPa, $p_l = 101.3$kPa.

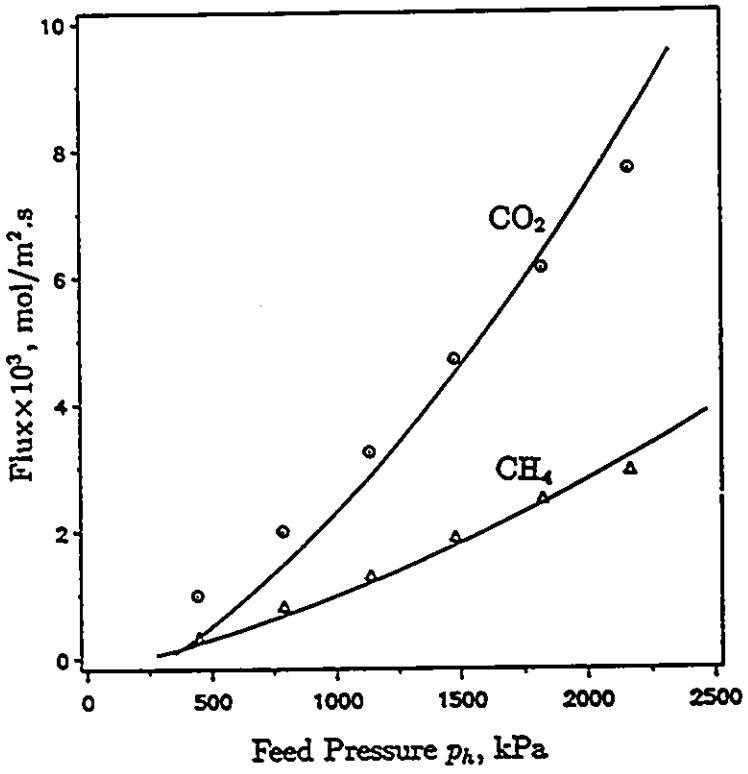

Figure 3.6(a): Effect of feed pressure on gas permeation through the CA membrane for which $r = 7.76 \times 10^{-10}$m. ($\odot$, Δ), experimental data; (———), calculated data. $X_{CO_2} = 0.501$, $p_l = 101.3$kPa.

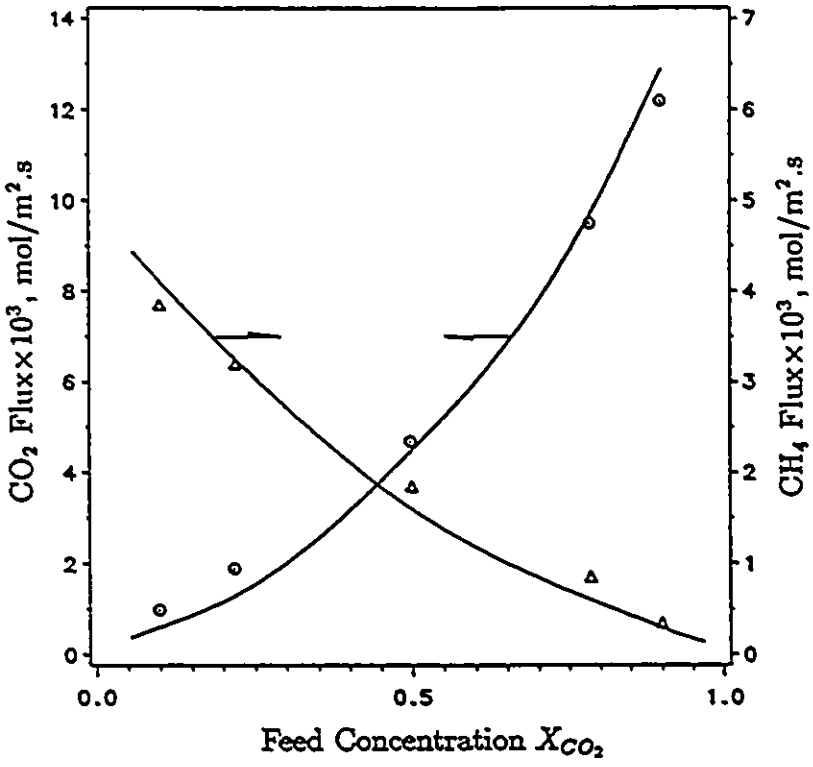

Figure 3.6(b): Effect of feed concentration on gas permeation through the CA membrane for which $r = 7.76 \times 10^{-10}$m. ($\odot$, $\triangle$), experimental data; (———), calculated data. $p_h = 1479$kPa, $p_l = 101.3$kPa.

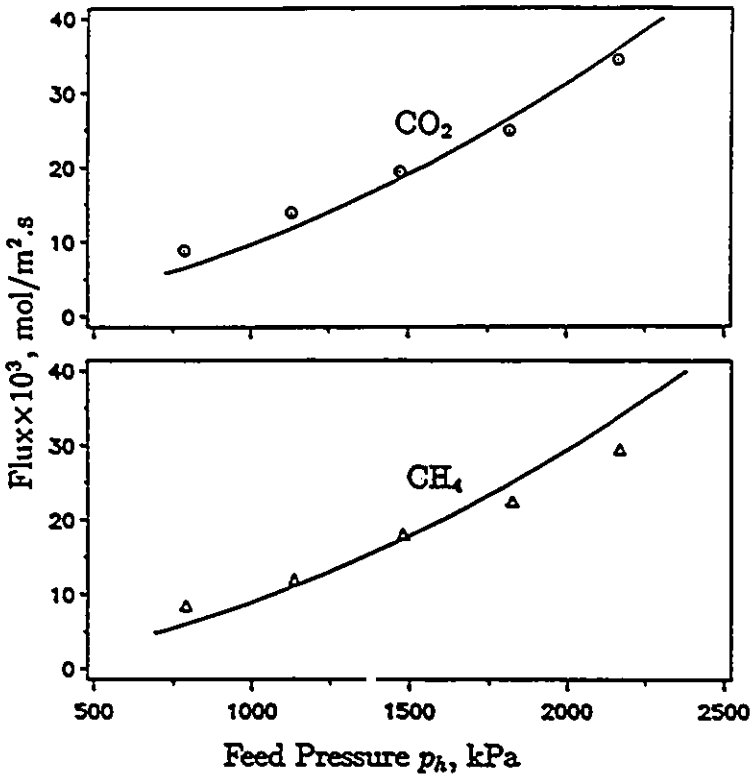

Figure 3.7(a): Effect of feed pressure on gas permeation through the CA membrane for which $r = 11.69 \times 10^{-10}$m. ($\odot$, $\triangle$), experimental data; (———), calculated data. $X_{CO_2} = 0.501$, $p_l = 101.3$kPa.

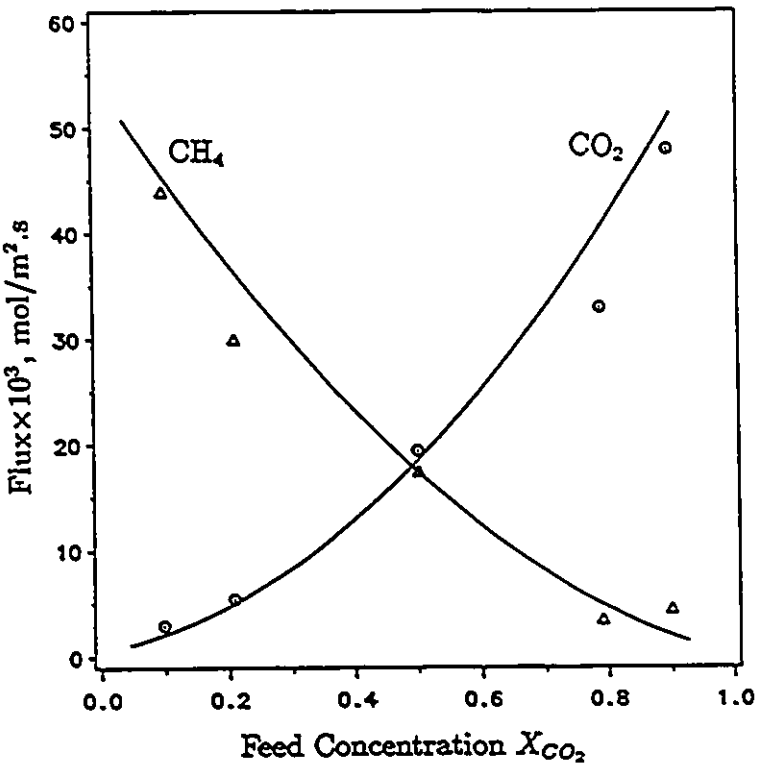

Figure 3.7(b): Effect of feed concentration on gas permeation through the CA membrane for which $r = 11.69 \times 10^{-10}$m. ($\odot$, $\triangle$), experimental data; (———), calculated data. $p_h = 1479$kPa, $p_l = 101.3$kPa.

concentration on permeate side is determined by the relative permeation rates of the components, an iteration method is used for the prediction of membrane performance with the aid of a computer. The calculation steps are as follows:

1. Assume a numerical value for CO_2 mole fraction in the permeate, Y_{CO_2}. Then, $Y_{CH_4} = 1 - Y_{CO_2}$

2. Calculate transmembrane average partial pressures and then surface viscosities of CO_2 and CH_4 using the following equations

$$p_{m,i} = (p_h X_i + p_l Y_i)/2$$
$$\mu_i = \exp[k p_{m,i}/(1 - K p_{m,i})]$$
$$i = CO_2, CH_4$$

3. Calculate permeation fluxes $Q_{t,i}$ using Eq.(3.1) or Eq.(3.3) as the case may be;

4. Calculate permeate composition $Y_i = Q_{t,i}/\sum Q_{t,i}$

5. Using the Y_i value calculated in step 4 go back to step 2. Repeat step 2, 3 and 4 until two consecutive Y_i values become equal;

6. Calculate permeability and separation factor

$$J_i = Q_{t,i}/\Delta p_i$$
$$\alpha = J_{CO_2}/J_{CH_4}$$

Figure 3.8 and 3.9 show the performance of a membrane having a pore radius of 5×10^{-10}m as a function of the feed pressure and the feed composition, respectively. The permeability of CO_2 tends to increase with an increase in the feed CO_2 concentration and the feed pressure. It is understandable because the increase in the average density of CO_2 molecules within the pore leads to an increase in the permeation flux under unit transmembrane pressure difference. It can be seen from

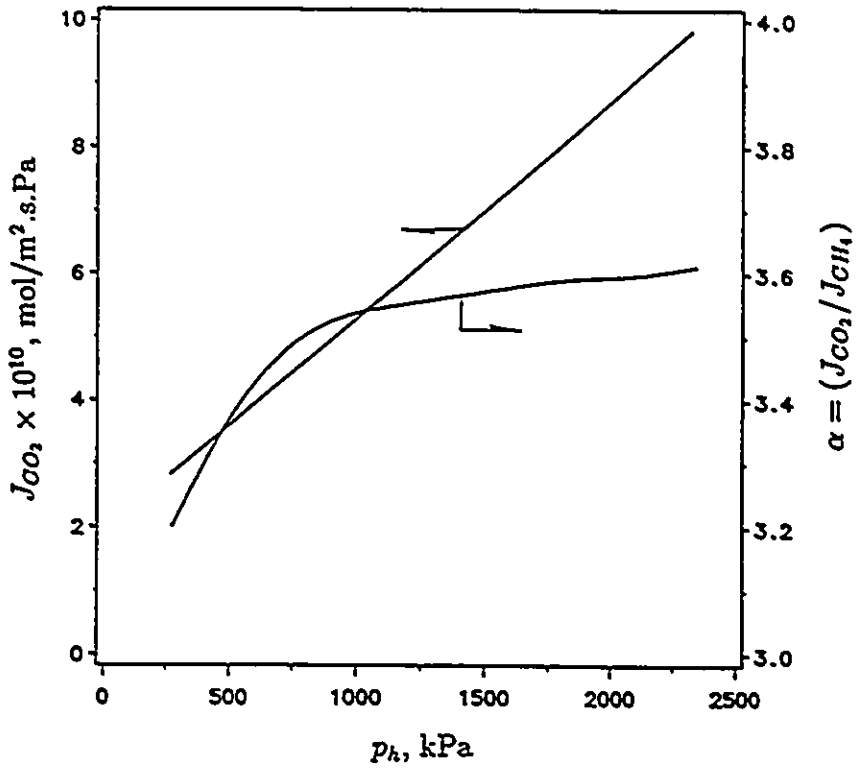

Figure 3.8: Model prediction — The effects of feed pressure on permeability and selectivity. $r = 5 \times 10^{-10}$m, $X_{CO_2} = 0.50$, $p_l =$ 101.3kPa.

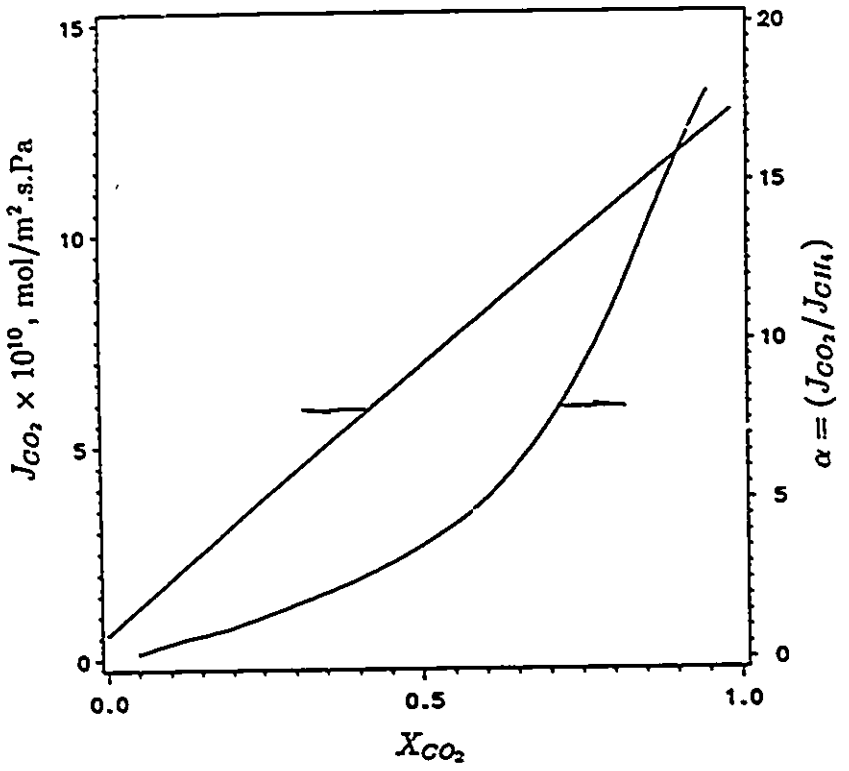

Figure 3.9: Model prediction — The effects of feed concentration on permeability and selectivity. $r = 5 \times 10^{-10}$m, $p_h = 1479$kPa, $p_l = 101.3$kPa.

Eq.(3.2) that the overall permeability is involved in two terms: Knudsen flow permeability and the surface flow permeability. The former is independent of the feed pressure and the feed concentration, while the latter is related to p_m/μ, the ratio of the average partial pressure across the membrane to the surface viscosity. Since the surface viscosity tends to increase as the average partial pressure increases, the change in surface flow permeability depends on the relative rate of the change in μ with respect to p_m. When the rate of increase in μ is not as fast as p_m, the surface flow permeability increases as p_m increases. In this case, the increase in the average partial pressure of CO_2 within the membrane p_{m,CO_2} resulting from either the increase in the feed pressure p_h, or the increase in the feed CO_2 concentration X_{CO_2} will cause an increase in the surface flow permeability of CO_2, and hence the overall CO_2 permeability.

On the other hand, the ideal separation factor expressed in terms of permeability ratio may increase or decrease depending on the relative magnitude of the changes in the permeabilities of CO_2 and CH_4. When the CO_2 and CH_4 permeabilities change at the same rate, the separation factor remains constant. The increase in the separation factor with the increases in p_h and X_{CO_2} shown in Figure 3.8 and 3.9 suggests that the CO_2 permeability increases faster than the CH_4 permeability.

The effect of permeate pressure p_l on the membrane performance is shown in Figure 3.10. When the permeate pressure increases, the permeabilities of both CO_2 and CH_4 increase, while the separation factor increases to a maximum and then tends to decrease because the percentage increase of permeabilities for CO_2 and CH_4 is different, as shown in Figure 3.11. When p_l is low, CO_2 permeability increases faster than CH_4 as p_l increases, causing an increase in the separation factor; When p_l is high, the CO_2 permeability increase is not as fast as CH_4, causing a decrease in

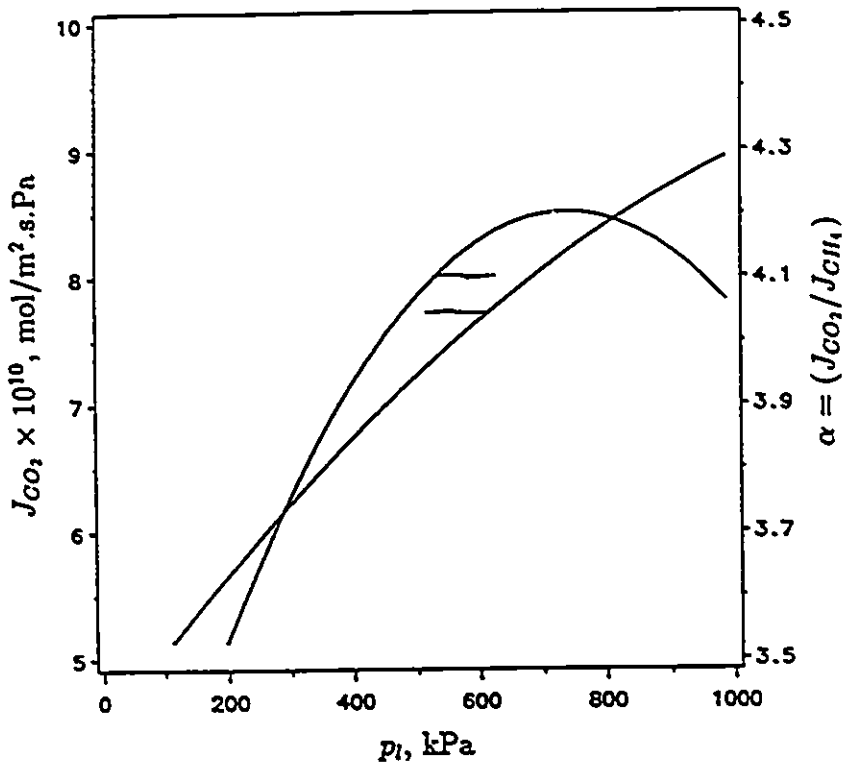

Figure 3.10: Model prediction — The effects of permeate pressure on permeability and selectivity. $r = 5 \times 10^{-10}$m, $X_{CO_2} = 0.50$, $p_h = 1479$kPa.

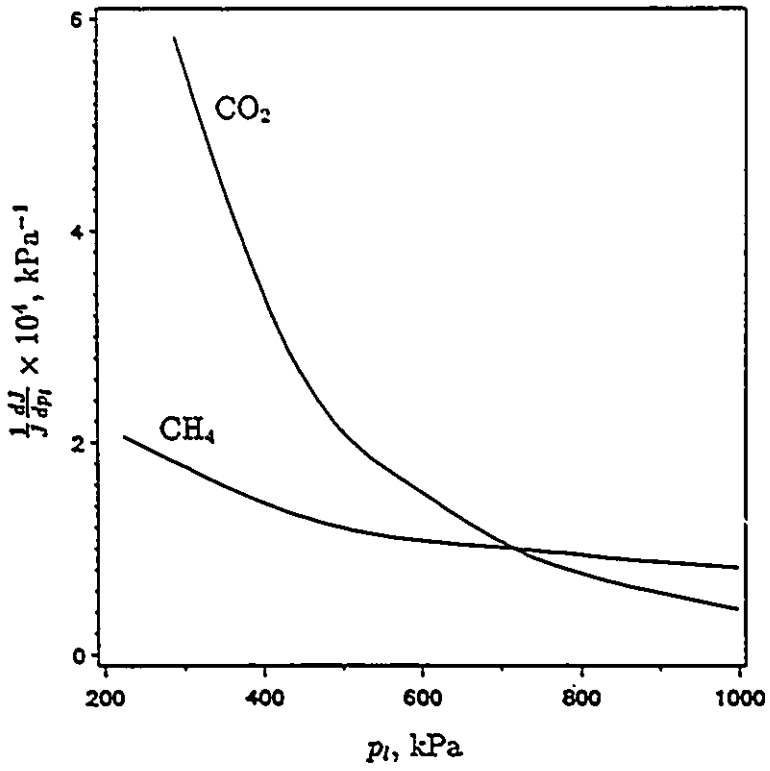

Figure 3.11: The effects of permeate pressure on the percentage increase of permeabilities. $r = 5 \times 10^{-10}$m, $X_{CO_2} = 0.50$, $p_h = 1479$kPa.

the separation factor. The point at which the percentage increase in permeabilities of CO_2 and CH_4 is identical, corresponds to the maximum separation factor. It is interesting to note that an increase in permeate pressure up to 720kPa can increase both permeability and separation factor. However, it should be noted that it is not necessarily a good policy to seek a high permeability or selectivity by raising the permeate pressure, because it is at the expense of sacrificing the available driving force for the permeation. Figure 3.12 shows that the permeation flux of CO_2 and the concentration of CO_2 in the permeate decrease with an increase in permeate pressure.

The pore radius has a significant influence on the membrane performance, as shown in Figure 3.13. Since CH_4 surface viscosity decreases much more rapidly than CO_2 as the pore size increases (refer to Figure 3.4), the separation factor diminishes rapidly as the pore size increases. In the range of pore size for which the calculation was performed, slip and viscous flows are not achieved. It is expected for pores of larger radii, slip flow or viscous flow becomes gradually more important. These two flow mechanisms lower the separation factor. Therefore, to achieve a high separation, the pore size on the membrane surface has to be sufficiently small so that surface flow is permitted and Knudsen flow is limited, while slip and viscous flows are eliminated.

It is well known that the permeabilities of individual components are usually different from those of pure components under the same transmembrane driving pressure. The possible reason is considered by some researchers as the concentration polarization or the competitive adsorption of permeating components on the membrane (Zhu and Liu, 1988). According to the pore flow model, the difference in permeability is attributed to the interaction between the permeating gas molecules. Figure 3.14 indicates that under the given operating conditions, the presence of CH_4 slows down CO_2 permeation. As a result the permeability ratio obtained from gas

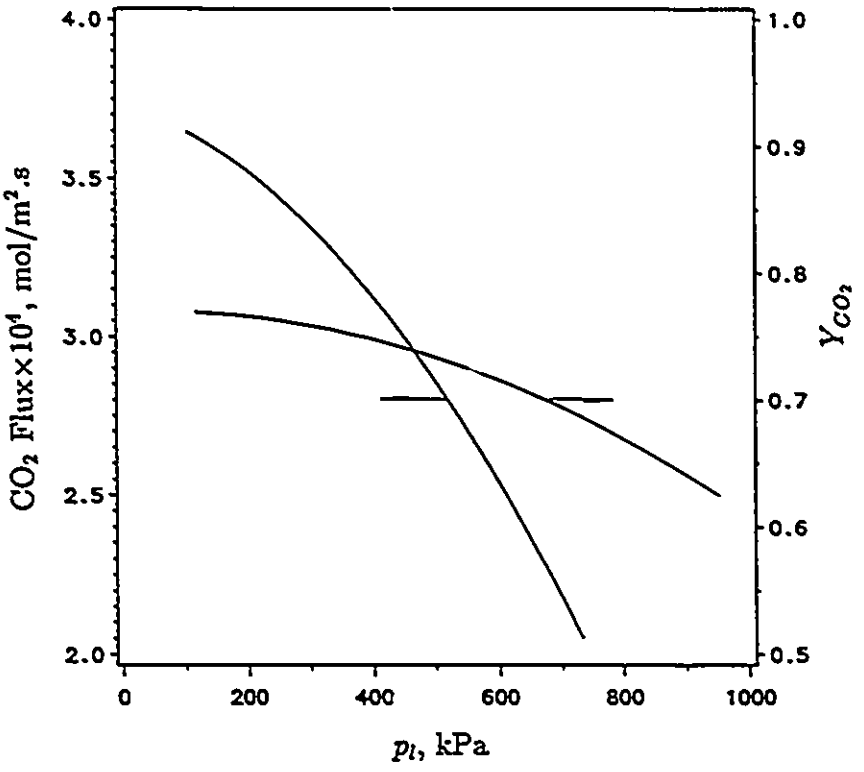

Figure 3.12: The effect of permeate pressure on the permeation flux and the permeate concentration. $r = 5 \times 10^{-10}$m, $X_{CO_2} = 0.50$, $p_h = 1479$kPa.

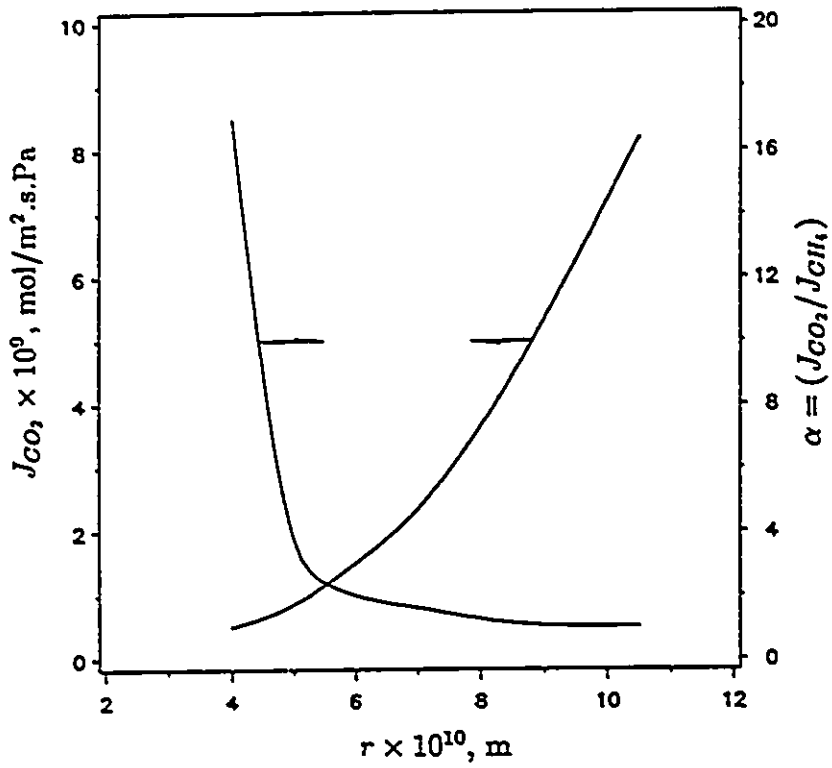

Figure 3.13: Model prediction — The effects of the membrane pore size on permeability and selectivity. $X_{CO_2} = 0.50$, $p_h = 1479$kPa, $p_l = 101.3$kPa.

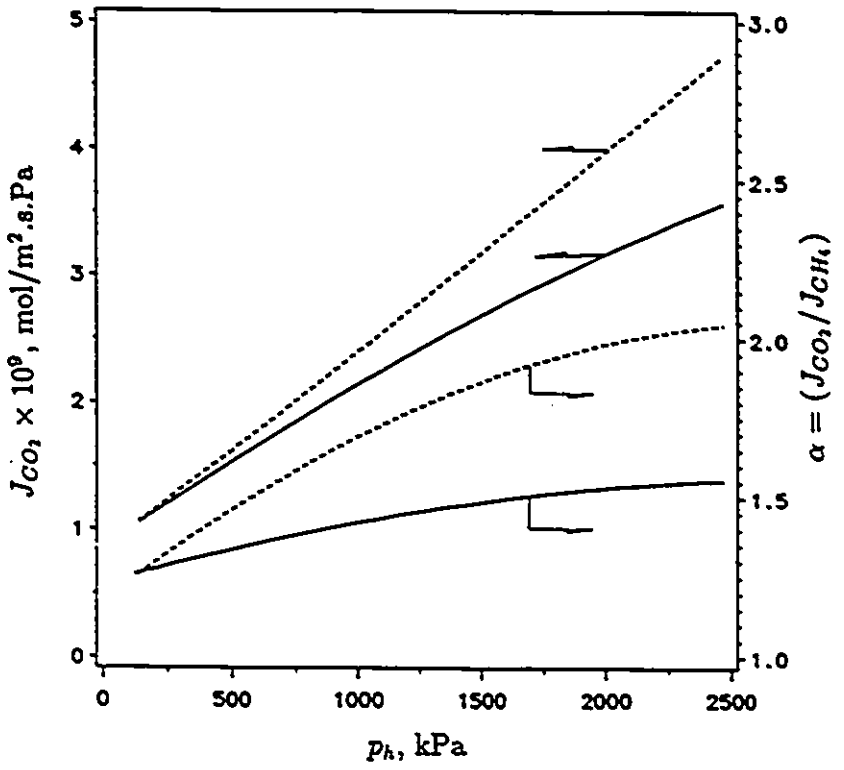

Figure 3.14: Comparison of permeabilities of pure gas and gas mixture. (——), predicted for gas mixture; (– – –), predicted for pure gas. $r = 7 \times 10^{-10}$m, $X_{CO_2} = 0.50$, $p_l = 101.3$kPa.

mixture differs from that obtained from pure gases. Though the pure gas permeability ratio is a convenient measure of the permeation selectivity, the interaction between the permeating components, particularly when it is strong, should be considered properly in the design of a membrane separation system.

3.4 Conclusions

The pore flow model initially used to describe the pure gas permeation process was extended to the transport of gas mixtures. The surface viscosity for the gas mixture permeation was calculated and correlated to the average partial pressure of the component gas across the membrane and the pore size of the membrane. The following conclusions can be drawn for the permeation of CO_2/CH_4 mixture through asymmetric cellulose acetate membranes:

1. The extended version of pore flow model is valid for the description of the gas mixture permeation;

2. The surface viscosity of a component in a gas mixture can be described by Eq.(3.5) empirically;

3. The membrane performance is affected by operating parameters including feed pressure, feed composition and permeate pressure;

4. The size of pores on membrane surface is crucial to the membrane performance. To get a high separation, the pore size has to be sufficiently small so that surface flow is permitted and Knudsen flow is limited, while slip and viscous flows are eliminated;

5. The permeabilities of individual components in a gas mixture differ from pure gas permeabilities under the same trans-membrane driving pressure.

3.5 Recommendation

The dependence of the surface viscosity on the pressure was empirically given by Eq.(3.5). The physical meanings of the equation and the parameters involved have to be clarified. For obtaining a more complete understanding of surface viscosities, studies with different membrane/gas systems are required. Several predicted results in this study have to be experimentally confirmed.

Chapter 4

Organic Vapor Separation from Air by Polyimide Membranes

The industries producing exhaust air streams contaminated by organic solvents have been under increasingly economic and regulatory pressure. In spite of various sources of organic emission, naphtha, toluene, xylene, perchloroethylene, trichloroethane, acetone, ethanol and methanol together represent almost eighty percent of the total emissions (Baker et al., 1987). The separation and recovery of organic vapors from waste air using membrane technology seems to be an attractive alternative to the conventional processes.

4.1 Background

Vapor–gas separation by means of membrane is different from gas–gas separation. Besides permeability and selectivity requirements, the ability of the polymer membrane to withstand organic vapor attack is also important. Although there is a great

amount of data in the literature concerning gas permeation through membranes, there are much fewer data on the permeation of organic vapors.

According to Baker et al. (1987), the appropriate membrane materials will be different for different organic vapors since a number of factors enter into material selection. However, most of experimental work reported were done using silicone rubber membranes. Kimmerle et al. (1988) and Paul et al. (1988) tested silicone rubber membrane coated on a porous polysulfone substrate. Behling (1986) chose polyetherimide as a support material because it is much more stable against organic vapors than polysulfone. To reduce the resistance of nonselective support to vapor permeation, the substrate has to be highly porous. However the pores must be sufficiently small so that they can be bridged by the coating material. The experimental data of Pinnau et al. (1988) indicate that the resistance of support layer is not negligible, and sometimes it is of the same order of magnitude as the resistance of the selective silicone rubber layer. Therefore the reported performance data of silicone rubber thin film composite membranes are quite different, depending on the properties of the support layer.

Although the silicone rubber membranes coated on a porous support were tested in laboratories and pilot plants, nothing was disclosed about the membrane preparation, perhaps for technical reasons. Referring to the Chemical Abstracts, no work has been reported up to now concerning vapor–gas separation using glassy polymer membranes, despite the fact that their excellent chemical and mechanical properties have been well known and that they have been widely used in commercial gas–gas mixture separations. In fact, it is because of these good properties that they are used as a support to silicone rubber membranes.

In this study, asymmetric polyimide membranes are to be explored for the sep-

aration of organic vapor from air. Attempts have been made to study the effects of parameters involved in the membrane preparation and develop membranes suitable for specific separation tasks. It might be expected that the permeability of air in the presence of an organic vapor would be different from the permeability obtained in the absence of the organic vapor. However, literature source (Baker et al., 1987) indicates that the effect of organic vapors on N_2 and O_2 permeabilities is very small. For convenience, membrane selectivities will be characterized in terms of the ratio of organic vapor permeability, which is obtained in the presence of air, and air permeability, which is obtained through a separate test run in the absence of organic vapors. The permeabilities of the membrane to hydrogen and nitrogen will also be tested. Their permeability ratio gives, to some extent, an indication of the size of pores on the membrane.

4.2 Experimental

Materials. Polyimide (PI 2080) was supplied by Upjohn Company. The polymer powder was dried at 120°C for 16 hours before use. A reagent grade N,N–dimethyl acetamide (DMAc), supplied by BDH Chemicals, served as solvent for the preparation of membrane casting solution. Lithium chloride (LiCl) from Fisher Scientific was dried at 140°C for 4 hours before used as an additive.

The following solvents were chosen to generate the simulated organic vapor streams in the permeation measurement: ethanol, acetone, *p*–xylene, 1,2–dichloroethane, benzene, chloroform and carbon tetrachloride from BDH Chemicals; methanol, hexane from Fisher Scientific; 1,2–dichloropropane from Matheson & Bell; and *m*–xylene from Phillips Petroleum Company.

Hydrogen, nitrogen and air gases were supplied by Air Products. The purities of hydrogen and nitrogen were specified as 99.95% and 99.997%, respectively. The total content of hydrocarbon impurities in the air was stated by the supplier to be less than 25ppm. All the gases were used without further purification.

Membrane Preparation. LiCl was dissolved in DMAc and then mixed with polyimide powder at a specified composition. The slurry was stirred at 40°C for about 30 hours to form a homogeneous casting solution. The polymer solution was cast on a clean Pyrex glass plate to a thickness of 250μm. The casting temperature and atmosphere was ambient (21.5°C, relative humidity $\leq$ 60%). The cast film, together with the glass plate, was placed in an oven at a specific temperature for a specific period of time to partially evaporate the solvent on the film surface. Then, the film, still on a glass plate, was immersed into ice cold water for 20min, during which time gelation took place and the film peeled off the plate. In order to prevent degradation of the polymer in water, the film was removed to an ethanol bath so that the water in the film was replaced by ethanol. After 24 hours of the solvent exchange, the film was air dried.

Apparatus and Procedures. The experimental setup shown schematically in Figure 4.1 was used to measure the organic vapor permeabilities. The permeation cell consisted of two detachable stainless steel parts. A porous stainless steel plate was embedded in one of the parts to support the membrane. The two parts of the cell were set in proper alignment with two rubber O-rings which were larger in diameter than the porous plate. A pressure tight seal was obtained by clamping the two parts tightly between two end plates. The effective area of the cell for permeation was 22.06cm^2.

Air went into a sintered stone ball immersed in an organic liquid to produce fine

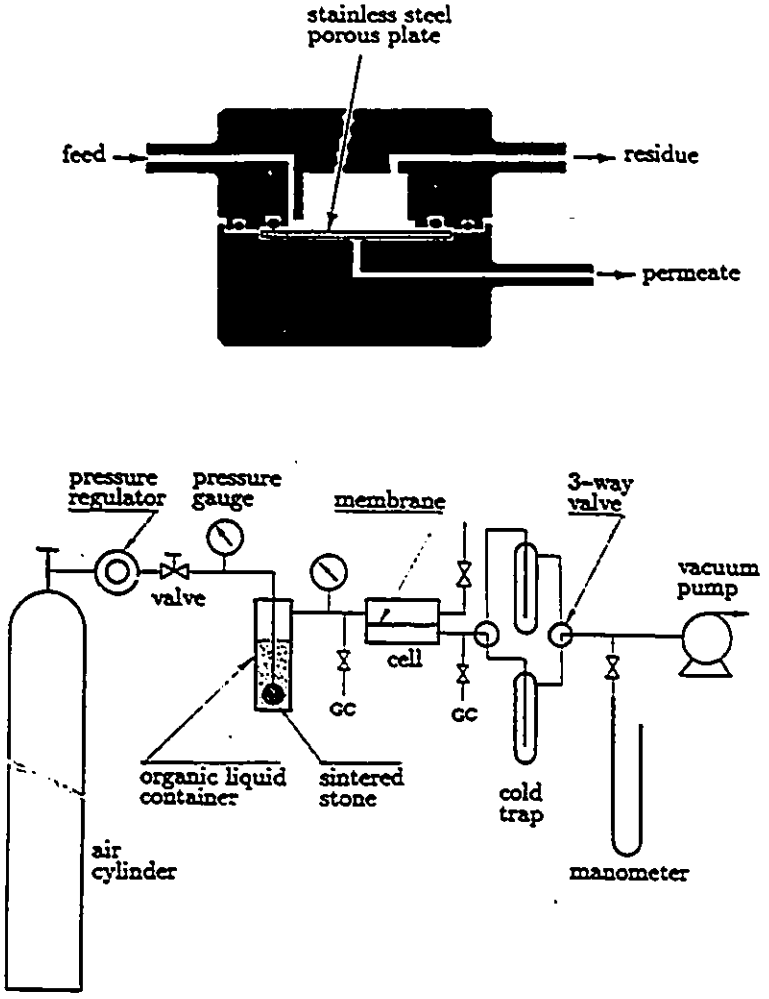

Figure 4.1: Test cell and flow diagram for organic vapor permeation measurement.

air bubbles that rose through the liquid. A mixture of air and organic vapor was obtained and then introduced into the permeation cell at a sufficiently high flow rate so that both concentration polarization in the direction vertical to the membrane surface and the change in concentration along the membrane surface were negligible. This means that the primary test data are local properties of the membrane.

A vacuum pump was applied on the permeate side to provide the necessary driving force for the permeation and to withdraw the permeated sample to a cold trap immersed in liquid nitrogen. The permeation rate of an organic vapor was determined by weighing the sample condensed and collected in a cold trap over a known period of time. The study was concerned with steady state permeation and separation. Approach to the steady state was monitored by measuring the permeation rate. Approximately 2 to 3 hours were required to reach the steady state.

Gas permeability measurement was performed in a traditional permeation cell, whose structure and the test diagram were shown in Figure 4.2. The permeate side was open to atmosphere and the permeation rate was determined by measuring the permeated gas flow rate using a bubble flow meter. The effective permeation area was $9.6cm^2$.

All the tests were carried out at laboratory temperature (22.5 ± 0.5^0C).

Determination of permeabilities. The permeability of pure air through the membrane is easily obtained

$$J_{air} = \frac{V}{A\,\Delta p}\,\frac{273.15}{273.15+22.5}\,\frac{1}{22400\times 60} \tag{4.1}$$

where V is the volumetric permeation rate of air measured by a bubble flow meter, ml/min.

It is reported that the effect of organic vapors on the nitrogen and oxygen perme-

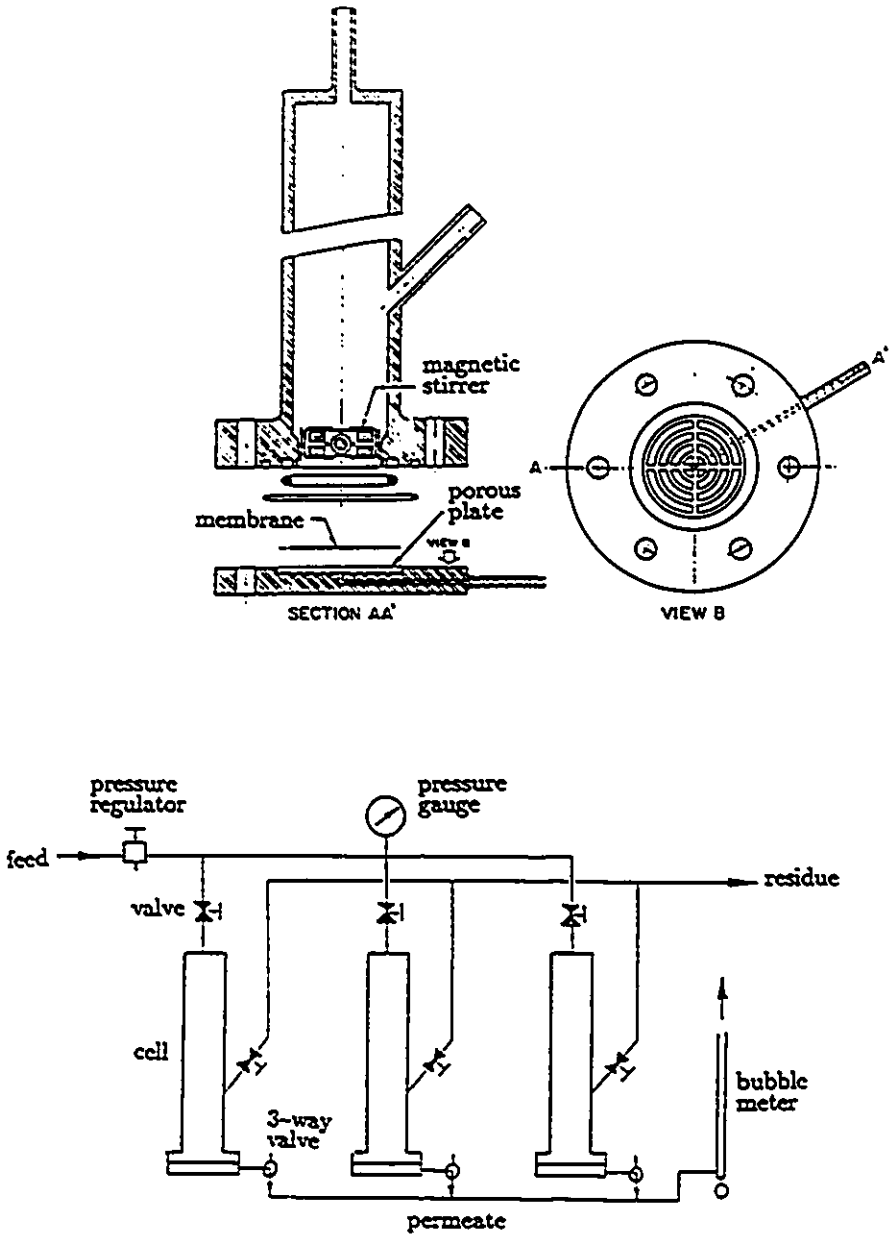

Figure 4.2: Test cell and flow diagram for gas permeation measurement.

abilities is very small (Baker et al., 1987). Assuming that the permeability of air is independent of the presence of organic vapors, the organic vapor permeability, J_{vap}, can be obtained by solving the following set of equations

$$Q_{vap} = J_{vap}(p_h X_{vap} - p_l Y_{vap}) \tag{4.2}$$

$$Q_{air} = J_{air}[p_h(1 - X_{vap}) - p_l(1 - Y_{vap})] \tag{4.3}$$

$$Y_{vap} = Q_{vap}/(Q_{vap} + Q_{air}) \tag{4.4}$$

where p_h, p_l, X_{vap} and Q_{vap} are known quantities from the organic vapor permeation experiment.

4.3 Results and discussion

4.3.1 Visual observations in membrane making procedure

When preparing the membrane casting solution, it is important to completely dissolve LiCl (additive) in DMAc (solvent) first, and then add polyimide powder slowly under stirring condition. Otherwise a block of polymer and salt would form, and the polymer was difficult to dissolve. The yellow suspension became dark brown when the polymer was dissolved in DMAc.

When the polymer content was less than 20wt% and the salt content ranged from zero to 6.2wt%, the resultant membranes were net-like and fragile. It is well known that in the wet process of membrane preparation, polymer concentration must be relatively high so that it can retain integrity during gelation. However, when polymer content was beyond 30wt% and salt content is 4.4wt%, the membrane broke into pieces during either the evaporation step or the gelation step. Fortunately,

25wt% of the polymer content could be used to obtain useful membranes. The latter polymer content was used throughout this study to test the effects of the membrane preparation parameters.

4.3.2 Effects of parameters involved in the procedure for membrane preparation

In order to test the effects of individual parameters involved in the procedure for membrane preparation on the resultant membrane performance, one of the parameters is changed while keeping the others constant. The test results are presented in Appendix C. Although the permeability for each organic vapor varies to different extents for different membranes, a common pattern in the permeability was observed, i.e.,

$$\left(\begin{array}{c} m-xylene \\ p-xylene \end{array}\right) > \left(\begin{array}{c} toluene \\ methanol \\ ethanol \end{array}\right) > \left(\begin{array}{c} benzene \\ CH_2ClCH_2Cl \\ CH_3CHClCH_2Cl \end{array}\right) > \left(\begin{array}{c} acetone \\ hexane \end{array}\right) > \left(\begin{array}{c} CCl_4 \\ CHCl_3 \end{array}\right) > air$$

Acetone and m-xylene are to be chosen in this study to test the effects of membrane preparation variables. It has to be noted that acetone and m-xylene represent a more permeable and a less permeable organic vapor, respectively, among the organic vapors under study. Moreover, they are two of the eight organic solvents producing most of the organic emissions into atmosphere.

Effect of salt content. Addition of salt to a casting solution has been studied for the preparation of reverse osmosis membranes. As shown in Figure 4.3, the concentration of LiCl in gelation bath was a function of gelation period, which was monitored using a CDM80 conductivity meter supplied by Radiometer A/S, Denmark. As gelation went on, the rate of salt leaving the film decreased. It is reasonable because

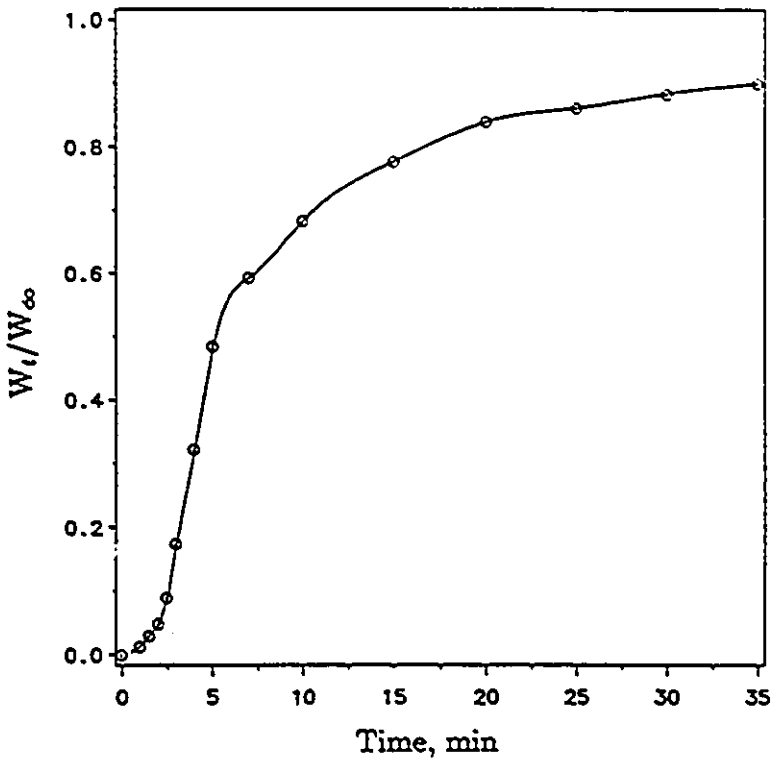

Figure 4.3: The rate curve for LiCl leaching out of the film in gelation bath.

Casting solution composition (wt%):
polyimide, 25; LiCl, 3.6; DMAc 71.4
Cast film thickness: 250μm
Gelation medium: ice cold water, 2^{0}C

the salt within cast film has to diffuse through the gelled polymer layer at the interface between the polymer and the gelation medium. The gelled polymer layer acts as a barrier to the salt leaching, and the rate of salt leaching gives some information concerning the thickness and porosity of the gelled polymer layer which is mainly responsible for the selective permeability of a membrane. It is shown that after 20 minutes of gelation, most of the salt has come out of the cast film for the particular case. Figures 4.4(a) and 4.4(b) show that the ratio of salt and polymer content in the casting solution has a significant effect on the permeability and selectivity of the membrane ultimately obtained. The detailed membrane making conditions are given in Table 4.1. As the salt concentration increases, the size and the effective number of pores on membrane surface increase. Consequently, permeabilities of the membrane to organic vapors increase.

The organic vapor permeability changes smoothly with the salt/polymer weight ratio, but the data for the permeability of air scatters. Therefore, the selectivity data scatters. The above results may be explained from the difference between gases and organic vapors. In comparison with organic vapors, the interaction between gas molecules and polymer material is weaker. Compared to surface flow, Knudsen, slip and viscous flows are not negligible. Because the gas molecular size is smaller than organic vapors, a small space in the membrane that can not accommodate an organic vapor molecule may be large enough to house gas molecules. Therefore, the gas permeability is more sensitive to a minor change in membrane structure than organic vapor.

Membrane selectivity depends on both organic vapor and air permeabilities. Though the selectivity data in Figures 4.4(a) and 4.4(b) are scattered, there is a tendency that a higher salt concentration in casting solution leads to a less selective

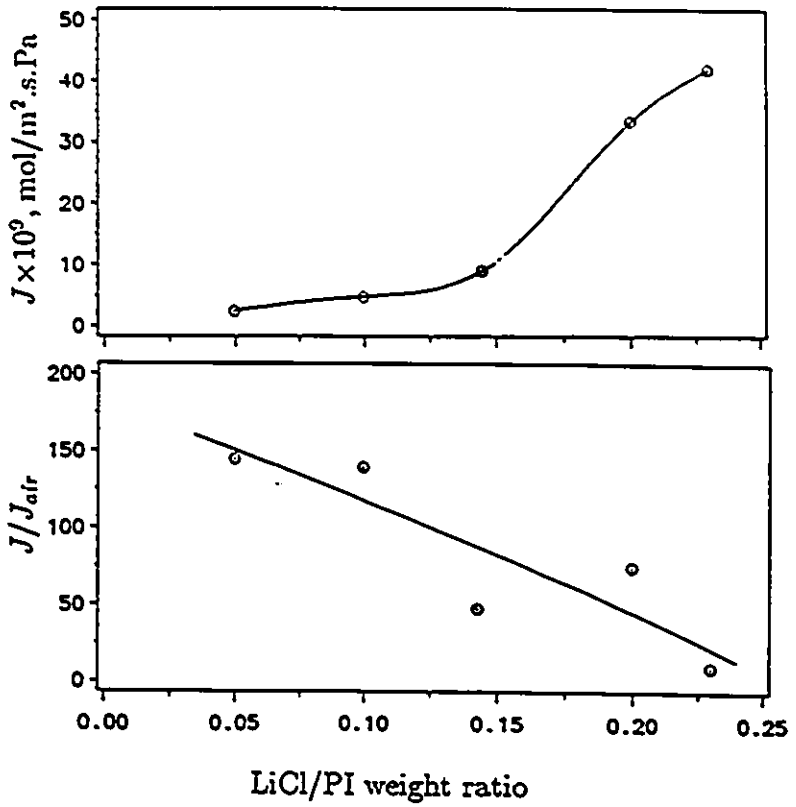

Figure 4.4(a): Effect of salt/polymer weight ratio in the casting solution on the permeability and selectivity of the membrane with respect to acetone. Membrane making conditions are given in Table 4.1.

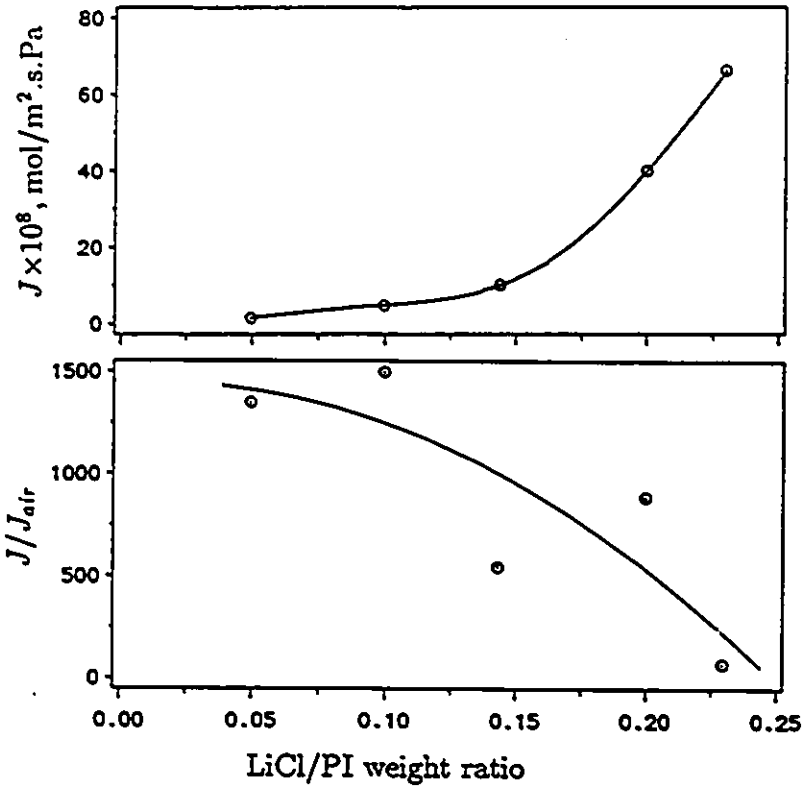

Figure 4.4(b): Effect of salt/polymer weight ratio in the casting solution on the permeability and selectivity of the membrane with respect to *m*-xylene. Membrane making conditions are the same as given for Figure 4.4(a).

Table 4.1: Details on membrane preparation

Casting solution composition	
	Polymer: polyimide, 25wt%
	Additive: LiCl*
	Solvent: DMAc*
Temperature of casting solution: 40°C	
Thickness of cast film: 250μm	
Film casting atmosphere: air	
Temperature of casting atmosphere: 22.5°C	
Solvent evaporation temperature: 85°C	
Solvent evaporation period: 20min	
Gelation medium: ice cold water, 2°C	
Gelation period: 20min	
Solvent for replacing water in the film: ethanol	
Solvent exchange period: 24hr	
Drying of membrane: air dried	

*LiCl wt% + DMAc wt% =75

membrane. When the polymer content is kept at 25wt% and the salt/polymer weight ratio in the casting solution increases from 0.05 to 0.23, permeabilities of acetone and *m*-xylene increase by about tenfold, but the permeability ratio of organic vapor relative to air decreases by nearly one order of magnitude. This means that as the salt content increases, the air permeability increases ten times faster than organic vapor.

The salt content is a very effective parameter to control the membrane performance. But, when the polymer content is kept as 25wt% and the salt/polymer weight ratio is above 0.25, it is difficult to make the casting solution homogeneous. On the other hand, if no salt is added, it is necessary to use a relatively high concentration of polymer in preparing the casting solution. Otherwise, the casting solution is too fluid to form a membrane by the phase inversion process. A high polymer concentration will significantly reduce permeability. Therefore permeability, selectivity and the ability to form a membrane must be considered simultaneously before deciding the amount of salt added to the casting solution.

Effect of evaporation temperature. Figure 4.5(a) and 4.5(b) show the effect of evaporation temperature during membrane formation on the performance of the resulting membranes. Increasing evaporation temperature results in a decrease in the permeability. Selectivity data are more scattered, but there is a definite tendency for the selectivity to decrease with an increase in the evaporation temperature.

The solvent evaporation temperature has a complex influence on the transport resistance of the membrane to a permeating component. Consider the three components in the casting solution: polymer, solvent and salt. (a) In the evaporation step, the local polymer concentration on the surface of the cast polymer film increases due to the loss of solvent, which tends to cause a low porosity of the membrane and hence a high permeation resistance. (b) Because of the solvent evaporation, the salt

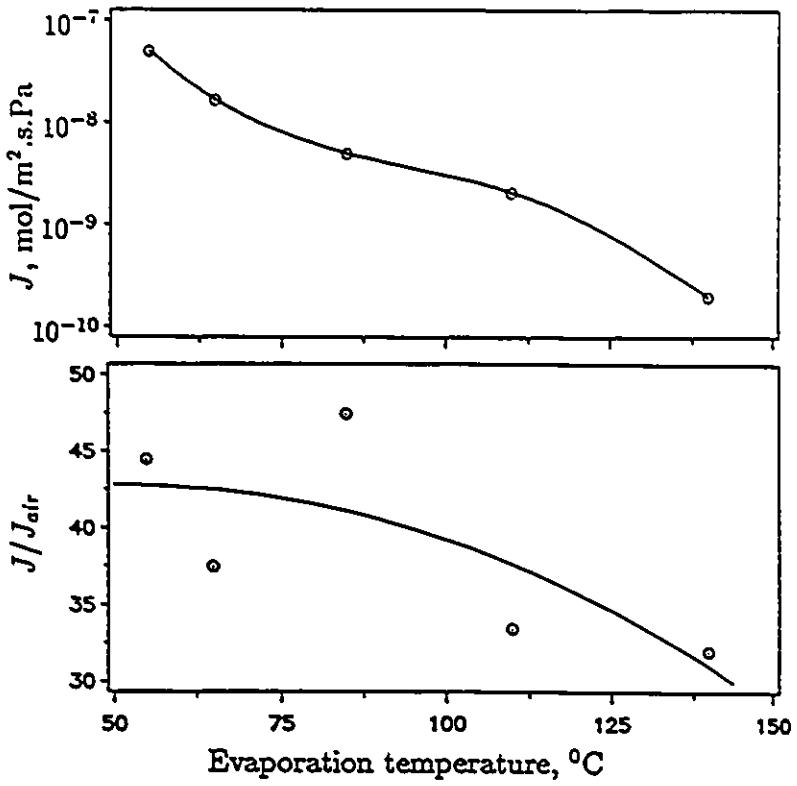

Figure 4.5(a): Effect of solvent evaporation temperature on the permeability and selectivity of the membrane with respect to acetone. Membrane making conditions are the same as given in Table 4.1 except the salt/polymer weight ratio is 0.144, and the solvent evaporation temperature is shown as above.

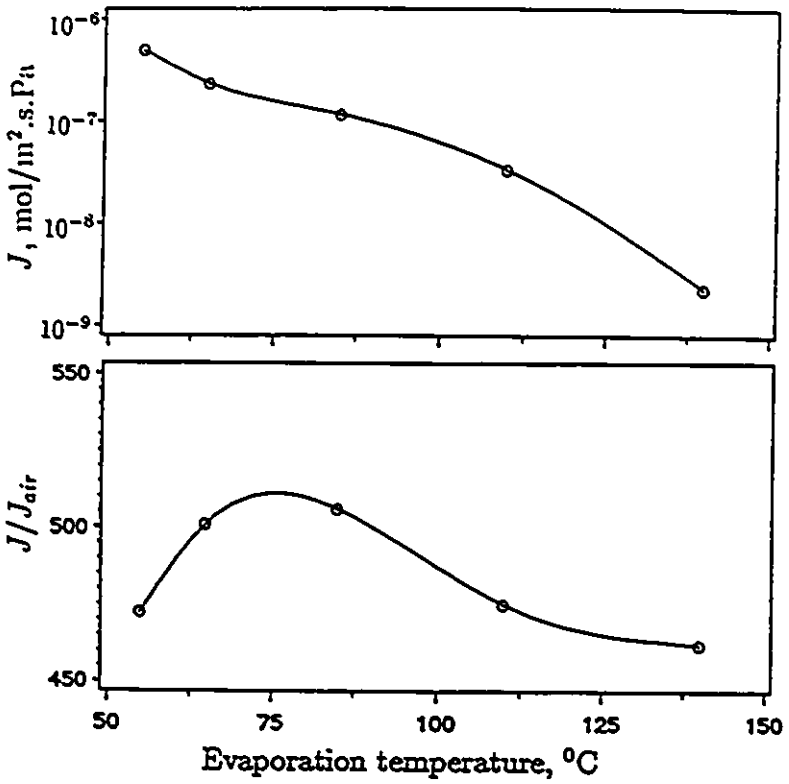

Figure 4.5(b): Effect of solvent evaporation temperature on the permeability and selectivity of the membrane with respect to *m*–xylene. Membrane making conditions are the same as given for Figure 4.5(a).

concentration on the cast film surface increases, which tends to increase porosity. (c) The higher the temperature is, the faster the evaporation takes place. When the temperature is very high, solvent evaporation rapidly rises to a level that solvent loss on the surface of the cast film can not be compensated by solvent diffusion from the interior to the film surface. The polymer soon comes out of the casting solution and forms a skin layer on the surface. Therefore, for a given period of evaporation, the effective thickness of a membrane will increase as temperature increases, resulting in a increase of permeation resistance. The overall effects determine the nature and magnitude of the change in permeability with evaporation temperature. If the combined effect is to increase the permeation resistance of the membrane, permeability will be reduced or vice versa.

The data presented in Figures 4.5(a) and 4.5(b) indicate that for the particular cases under study, an increase in solvent evaporation temperature significantly reduces the permeability of organic vapor, but the permeability ratio of organic vapor relative to air is less affected. When the evaporation temperature changes from 55°C to 140°C, the permeability of organic vapor undergoes a decrease of nearly two orders of magnitude. However, the vapor/air permeability ratio decreases by only 40% for acetone and 10% for *m*–xylene. It is obvious that the air permeability is also significantly reduced by a high evaporation temperature. The above results suggest that a lower evaporation temperature is preferable to prepare a membrane of high permeability and high selectivity. But, because of the relatively high boiling point of solvent DMAc, a low evaporation temperature leads to a high porosity on the membrane, resulting in insufficient mechanical strength of the membrane.

Effect of evaporation time. As indicated in Figure 4.6(a) and 4.6(b), the membrane performance is influenced by solvent evaporation period. Increasing evap-

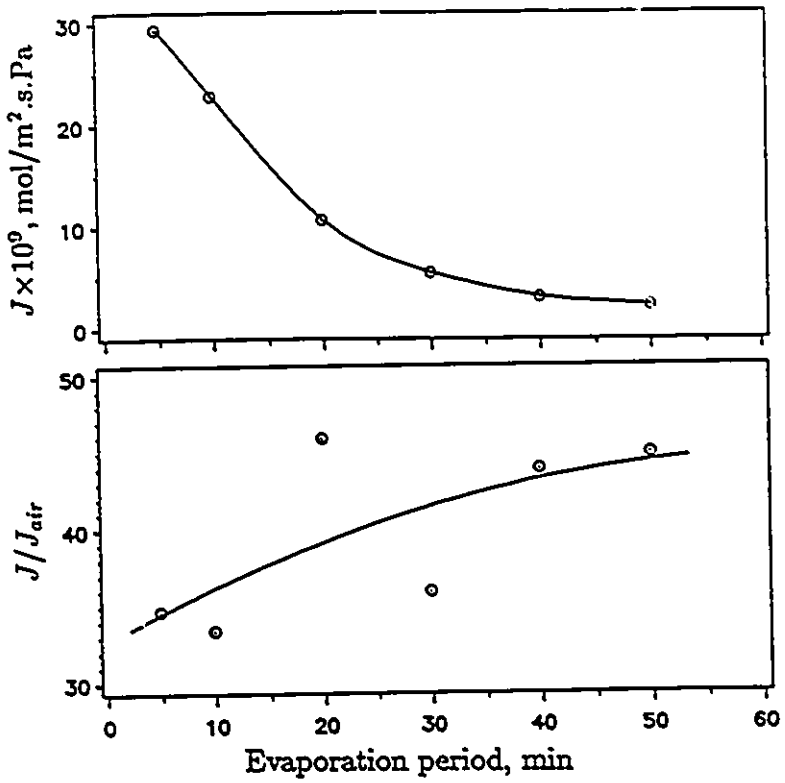

Figure 4.6(a): Effect of solvent evaporation period on the permeability and selectivity of the membrane with respect to acetone. Membrane making conditions are the same as given in Table 4.1 except the salt/polymer weight ratio is 0.144, and the solvent evaporation time is shown above.

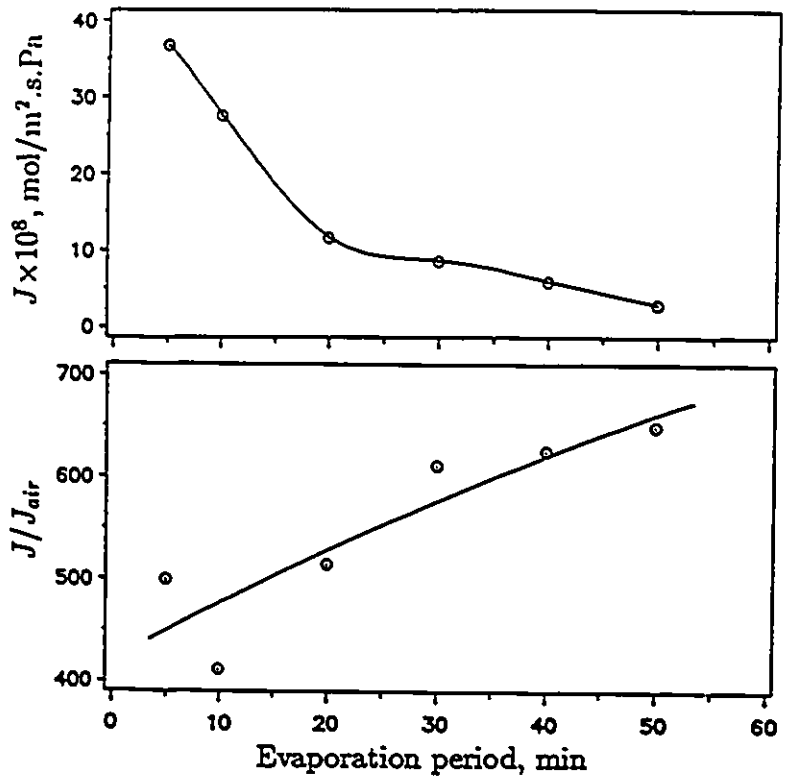

Figure 4.6(b): Effect of solvent evaporation period on the permeability and selectivity of the membrane with respect to *m*–xylene. Membrane making conditions are the same as given for Figure 4.6(a).

oration time prior to immersion of the cast film in the gelation bath causes a decrease in permeability. This result is consistent to the observation of Kesting (1985), who tested water permeation rate through cellulose acetate membranes. It is understandable in view of the fact that the permeability depends mainly on the thickness of skin layer, the size and the number of pores on the membrane surface. As evaporation period increases, the skin layer becomes thicker and the possibility of existence of big pores on the membrane surface is small.

When the permeability of a membrane to organic vapors varies due to the variation of the membrane porous structure, the permeability to air also undergoes a similar change. Hence the permeation selectivity to an organic vapor and air, characterized in terms of their permeability ratio, changes to a lesser extent. The change may be negative or positive, depending on the relative rate of changes in the permeabilities of the organic vapor and air. The increase in the vapor/air permeability ratio, as shown in Figure 4.6(a) and 4.6(b), indicates air permeability is more significantly affected by evaporation period than the organic vapor permeability.

Comparing Figure 4.5 and 4.6, the solvent evaporation temperature and the evaporation period have similar but not the same influence on the membrane performance. The former determines the solvent evaporation rate, and they two together determine the amount of solvent evaporated during the evaporation step. Both of them are important to control the membrane morphology and hence the performance of the membrane.

4.3.3 Correlation between permeability and solubility parameter

For all the membranes tested, the permeability ratio of hydrogen to nitrogen is in the range of 1.5 to 1.8, less than the one calculated by Knudsen flow mechanism, which is 3.74. This indicates that some pores exist on the membrane surface which permit slip flow and/or viscous flow. However, organic vapor permeability is much higher than the gas permeability. The reason may be that organic vapor has a strong interaction with the membrane material, and the surface flow of the adsorbed organic vapor molecules on the wall of pores dominates. Because of the adsorption layer, transport area within the pore for other flow mechanisms is reduced.

According to the surface force and pore flow model, for a given membrane, permeability is affected by the size of penetrant and the interaction between the membrane and the permeating molecules. Generally speaking, as the size of a penetrant increases, the sorption on a polymer material increases and the mobility through the pores within a membrane decreases. Either preferential sorption on membrane surface or fast transport through membrane may contribute to the high permeability. It has been observed that polymer morphology is affected by the sorption of an organic vapor, causing an increase in both the sorptive capacity of the polymer and the mobility of the organic vapor within the polymer (Blackadder and Keniry, 1972; Laine and Osburn, 1971). It is well known that the sorption of liquids by polymer shows a maximum where the solubility parameters of the liquid and the polymer are identical. Pilato et al. (1975) observed a maximum in CO_2 permeability through different polymer membranes where solubility parameter of CO_2 is close to that of the polymer. It seems that the sorption property is more important to the permeability of a condensable component. It is therefore desirable to observe the relationship be-

tween the organic vapor permeability and its solubility parameter, which is shown in Figure 4.7.

Because the repeat unit of the polyimide material used in the study is not known, it is difficult to obtain the solubility parameter of the polymer. Now that N,N dimethyl acetamide (DMAc) serves as solvent to the polymer in this study, the solubility parameter of DMAc should be close to that of the polyimide material. Referring to Figure 4.7, there seems a tendency that the permeability of an organic vapor through the polymer membrane depends on the solubility parameter difference between the organic vapor and the polymer. However, more and further work should be done to test the correlation before a universal conclusion can be made.

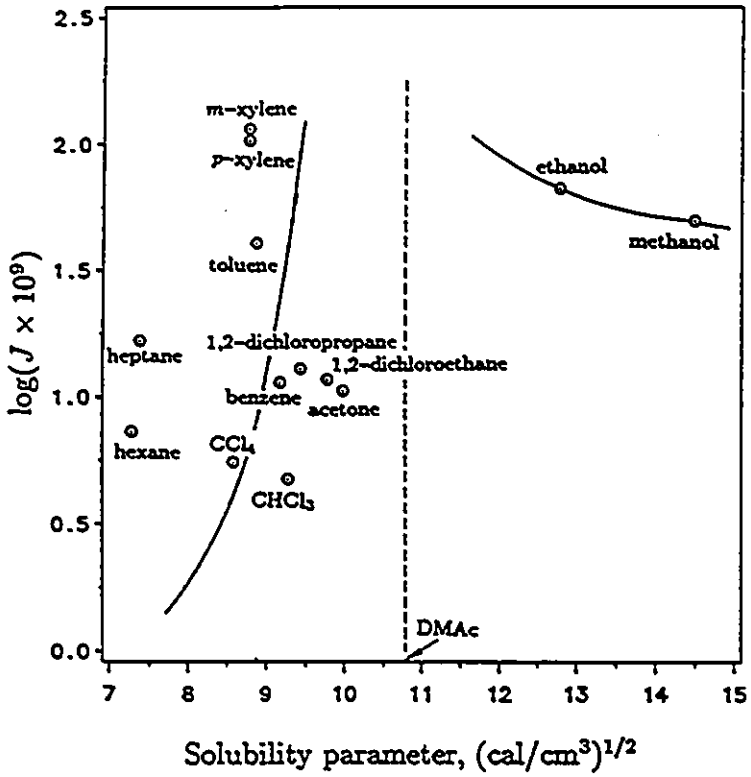

Figure 4.7: Organic vapor permeability versus solubility parameter. Membrane making conditions are the same as given in Table 4.1 except the salt/polymer weight ratio is 0.144.

4.4 Conclusions

The dry asymmetric membranes prepared by the phase inversion technique are studied for the separation of organic vapors from air. It is concluded from the work that:

1. The dry asymmetric polyimide membrane is preferentially permeable to organic vapors when feed air–organic vapor mixtures are tested;

2. The membrane performance is affected strongly by the conditions of membrane preparation. Increasing the content of salt or reducing the temperature and period for solvent evaporation will increase organic vapor permeability;

3. For a given membrane the permeability of organic vapor increases with a decrease in the difference of solubility parameter between the organic compound and the membrane material.

4.5 Recommendation

The effects of operating parameters such as feed concentration, permeate pressure (vacuum), and operation temperature on the membrane performance should be studied to get a complete understanding of the process. A simulated mixture of organic vapor and air has to be tested so as to evaluate the economics of the process. A theoretical description of organic vapor permeation through the membrane is to be developed.

Bibliography

[1] Agrawal, J.P. and S. Sourirajan, "High flux freeze–dried cellulose acetate membranes as microporous barriers in gas permeation and separation", *J. Appl. Polym. Sci.*, 14,1303(1970).

[2] Backhouse, I.W., "Recovery and purification of industrial gases using Prism separators", in *Proc. 4th BOC Priestley Conf.*, Leeds (1986), p265.

[3] Baker, R.W., N. Yoshioka, J.M. Mhor and A.J. Khan, "Separation of organic vapors from air", *J. Membrane Sci.*, 31,259(1987).

[4] Baldus, W. and D. Tillman, "Conditions which need to be fulfilled by membrane systems in order to compete with existing methods of gas separation", *Proc. 4th BOC Priestley Conf.*, Leeds (1986), p26.

[5] Beaver, E.R., P.V. Bhat and D.S. Sarcia, "Integration of membrane with other air separation technologies", *AIChE Symp. Ser.* 261, 113(1988).

[6] Behling, R.D., "Separation of hydrocarbon vapors from air", *Proc. 6th Annual Membr. Tech. Planning Conf.*, Session V–4, Cambridge, MA (1988).

[7] Blackadder, D.A. and J.S. Keniry, "The morphological consequences of annealing high density polyethylene in solvents", *J. Appl. Polym. Sci.*, 16,1261(1972).

[8] Chen, Y., "A modified resistance model for gas permeation through composite membranes", Seminar presented at Industrial Membrane Research Institute, University of Ottawa, February 1989.

[9] Chen, Y., A. Fouda and T. Matsuura, "A study on dry cellulose acetate membrane for the separation of carbon dioxide and methane mixtures", in *Advances in Reverse Osmosis and Ultrafiltration*, T. Matsuura and S. Sourirajan (Eds.), National Research Council of Canada, Ottawa (1989), p259.

[10] Chern, R.T., W.J. Koros, H.B. Hopfenberg and V.T. Stannett, "Material selection for membrane based gas separations", in *Materials Science of Synthetic Membranes*, D.R. Lloyd (Ed.), ACS, Washington DC (1985), p25.

[11] Chiou, J.S., Y. Maeda and D.R. Paul, "Gas and vapor sorption in polymers just below T_g", *J. Appl. Polym. Sci.*, 30, 4019(1985).

[12] Cifuentes, M., C.L. Lee, H. Chapman, K. Lee and K. Ulman, "Investigation of structure – permeability relationships in silicone polymers", in *Synthetic Membranes*, M.B. Chenoweth (Ed.), MMI Press (1986), p251.

[13] Conover, S.P., "Novel gas separation membrane modules", *Proc. 4th Annual Membr. Tech. and Planning Conf.*, Cambridge MA (1986), p188.

[14] Fain, D.E., "Gas separation processes: technology/business review", *Proc. 6th Annual Membr. Tech. and Planning Conf.*, Session V–5, Cambridge MA (1988).

[15] Finken, H., "Asymmetric membrane for gas separations", in *Materials Science of Synthetic Membranes*, D.R.Lloyd (Ed.), ACS, Washington DC (1985), p245.

[16] Fouda, A.E., T. Matsuura and A. Lui, "Permeation of gas mixtures in cellulose acetate membranes. Practical approach to predict the permeation rate of CO_2/CH_4 mixtures", presented at *The 5th Symp. Sep. Sci. Tech. for Energy Applications*, Knoxville, TN (1987).

[17] Gantzel, P.K. and U. Merten, "Gas separation with high flux cellulose acetate membranes", *Ind. Eng. Chem. Process Des. Dev.*, 9, 331(1970).

[18] Generon, "Generon announces gas separation breakthrough", *Membrane Separation & Technology News*, 7(10), 1(1989).

[19] Gottschlich, D.E., D.L. Roberts and J.D. Way, "A theoretical comparison of facilitated transport and solution–diffusion membrane modules for gas separation", *Gas Sep. & Purification*, 2, 71(1988).

[20] Haggin, J., "New generation of membranes developed for industrial separations", *Chem. Eng. News*, June 1988, p7.

[21] Hakuta, T., K. Haraya, K. Obata, Y. Shindo, N. Ito and H. Yoshitome, "A state of the art of gas membrane separation in C_1 chemistry project", *Proc. Int. Cong. Membranes*, Tokyo(1987), p564.

[22] Henis, J.M.S. and M.K. Tripodi,"Multicomponent membranes for gas separations", *US Patent 4,230,465*, 1980a.

[23] Henis, J.M.S. and M.K.Tripodi,"A noval approach to gas separations using composite hollow fiber membranes", *Sep. Sci. Tech.*, 15, 1059(1980b).

[24] Henis, J.M.S. and M.K. Tripodi,"Composite hollow fiber membranes for gas separation: the resistance model approach", *J. Membrane Sci.*, 8, 233(1981).

[25] Hwang, S.T. and J.M. Thorman."The continuous membrane column", *AIChE J.*, 26, 558(1980).

[26] Kesting, R.E., *Synthetic Polymeric Membranes*, McGraw Hill, New York, NY (1971).

[27] Kesting, R.E., "Phase inversion membranes", in *Materials Science of Synthetic Membranes*, D.R.Lloyd (Ed.), ACS, Washington, DC (1985), p131.

[28] Kim, T.H., W.J. Koros, G.R. Husk and K.C. O'Brien, "Relationship between gas separation properties and chemical structure in a series of aromatic polyimides", *J. Membrane Sci.*, 37, 45(1988).

[29] Kimmerle, K., C.M. Bell, W. Gugernatsch and H. Chmiel, "Solvent recovery from air", *J. Membrane Sci*, 36, 477(1988).

[30] Koros, W.J., "Membrane-based gas separations: data base and models for glassy polymers", paper presented at Sunriver membrane conference, Sunriver, Sept. 1983.

[31] Krishna, R., "A unified theory of separation processes based on irreversible thermodynamics", *Proc. 4th BOC Priestley Conf.*, Leeds (1986), p64.

[32] Laine, R. and J.O. Osburn, "Permeability of polyethylene film to organic vapors", *J. Appl. Polym. Sci.*, 15, 327(1971).

[33] Laverty, B.W. and J.G. O'Hair, "Application of membrane technology in the gas industry", *Proc. 4th BOC Priestley Conf.*, Leeds (1986), p291.

[34] Lloyd, D.R., "Membrane materials science: an overview", in *Materials Science of Synthetic Membranes*, D.R. Lloyd (Ed.), ACS, Washington, DC (1985), p1.

[35] Long, V.T., B.S. Mihas, T. Matsuura and S. Sourirajan, "Gas chromatographic method for measurement of gas sorption on polymer materials", *J. Colloid Interface Sci.*, 125.478(1988).

[36] Lonsdale, H.K., "The growth of membrane technology", *J. Membrane Sci.*, **10**, 81(1982).

[37] Lonsdale, H.K., "Membrane separation technology in the 1980s", in *Membrane and Ultrafiltration Technology: Development Since 1981*, S. Torrey (Ed.), Noyes Data Co., Park Ridge (1984), p419.

[38] MacLean, D.L., "The structure of gas separation technology", *Proc. 4th BOC Priestley Conf.*, Leeds (1986), p382.

[39] MacLean, D.L., C.E. Prince and Y.C. Chae, " Energy saving modification in ammonia plant", *Chem. Eng. Prog.*, May 1980, p98.

[40] Manos, P., "Gas separation membrane drying with water replacement liquid", *US Patent 4,080,744*, 1978.

[41] Matson, S.L., J. Lopez and A. Quinn, "Separation of gases with synthetic membranes", *Chem. Eng. Sci.*, 38, 503(1983).

[42] Matsuura, T. and S. Sourirajan, *Recent Progress in Membrane Separation Processes*, National Research Council of Canada, Ottawa (1988).

[43] Matsuura, T. and S. Sourirajan, "Preferential sorption – capillary flow mechanism and surface force – pore flow model: Applicability to different membrane separation processes", in *Advances in Reverse Osmosis and Ultrafiltration*, T. Matsuura and S. Sourirajan (Eds.), NRCC, Ottawa (1989), p139.

[44] Mazur, W.H. and M.C. Chan, "Membranes for natural gas sweeting and carbon dioxide enrichment", *Chem. Eng. Prog.*, 78, 38(1982).

[45] Nakagawa, T., T. Saito, Y. Kojima, H. Nakano and A. Higuchi, "Stabilized poly(1-trimethyl silyl-1-propyne) membranes with high gas permselectivity", *Proc. Int. Cong. Membranes*, Tokyo(1987), p512.

[46] Nippon Kokan, "Hydrocarbon vapor recovery with membrane technology", *Technical Bulletin*, Nippon Kokan, Tokyo (1987).

[47] Pan, C.Y. and H.W. Habgood, "Gas separation by permeators – Part 1: Calculation methods and parametric analysis", *Can. J. Chem. Eng.*, **56**, 197(1978a).

[48] Pan, C.Y. and H.W. Habgood, "Gas separation by permeators – Part 2: Effect of permeate pressure drop and choice of permeate pressure", *Can. J. Chem. Eng.*, **56**, 210(1978a).

[49] Paul, H., C. Philipsen, F.J. Gerner and H. Strathmann, "Removal of organic vapor from air by selective membrane permeation", *J. Membrane Sci.*, **36**,363(1988).

[50] Perrin, J.E. and S.A. Stern,"Modeling of permeators with two different types of polymer membranes", *AIChE J.*, **31**, 1167(1985).

[51] Pilato, L.A., L.M. Litz, B. Hargitay, R.C. Osburn, A.G. Farham, J.H. Kawakami, P.E. Fritze and G.E. McGrath, "Polymers for permselective membrane gas separation", *Polymer Preprints*, **16**(2), 41(1975).

[52] Pinnau, I., J.G. Wijamans, I. Blume, T. Kuroda and K.V. Peinemann, "Gas permeation through composite membranes", *J. Membrane Sci.*, **37**, 81(1988).

[53] Rangaranjan, R., M.A. Mazid, T. Matsuura and S.Sourirajan, "Permeation of pure gases under pressure through asymmetric porous membranes. Membrane characterization and prediction of performance", *Ind. Eng. Chem. Proc. Des. Dev.*, *23*, 79(1984).

[54] Raucher, D. and M.D. Sefcik, "Gas transport and cooperative main-chain motions in glassy polymers", in *Industrial Gas Separations*, T.E. Whyte, Jr., C.M. Yon and E.H. Wagener (Eds.), ACS, Washington, DC (1983), pS9.

[55] Reuvers, A.J. and C.A. Smolders, "Asymmetric membranes prepared by phase inversion precipitation", *Proc. Int. Cong. Membranes*, Tokyo (1987), p11.

[56] Ruf, A. and S. Egli, "Application of gas separation shown through the purification of landfill gas", *Gas Sep. & Purification*, 2, 91(1988).

[57] Schell, W.J. and C.D. Houston, "Process gas with selective membranes", *Chem. Eng. Prog.*, 78, 33(1982).

[58] Schendel, R.L., "Separation of acid gas and hydrocarbon", *Proc. 4th BOC Priestley Conf.*, Leeds (1986), p311.

[59] Schendel, R.L., "Using the membrane for the separation of acid gases and hydrocarbons", *Chem. Eng. Prog.*, 80, 39(1984).

[60] Scott, J., *Membrane and Ultrafiltration Technology: Recent Advances*, Noyes Data Corp., Park Ridge, NJ (1980).

[61] Sengupta, A. and K.K. Sirkar, "Membrane gas separation", in *Progress in Filtration and Application*, J. Wakeman (Ed.), Elsevier, (1986), p289.

[62] Sirkar, K.K., "Asymmetric permeators — conceptual study", *Sep. Sci. Tech.*, 15, 1091(1980).

[63] Sourirajan, S., *Reverse Osmosis*, Academic Press (1970).

[64] Sourirajan, S., "A unified approach to membrane separations", *Proc. 7th Annual Membr. Tech and Planning Conf.*, Cambridge MA (1989), p472.

[65] Sourirajan, S. and T. Matsuura, *Reverse Osmosis and Ultrafiltration Process Principles*, National Research Council of Canada, Ottawa (1985).

[66] Stanley, M., "Thomas Graham and gaseous diffusion", *Proc. 4th BOC Priestley Conf.*, Leeds (1986), p161.

[67] Stern, S.A., "New developments in membrane processes for gas separations", in *Synthetic Membranes*, M.B. Chenoweth (Ed.), MMI Press (1986), p1.

[68] Stern, S.A., "The separation of gases by selective permeation", in *Membrane Separation Processes*, P. Meares (Ed.), Elsevier, (1976), p295.

[69] Strathmann, H., "Synthetic membranes and their preparations", in *Synthetic Membranes: Science, Engineering and Applications*, P.M. Bungay, H.K. Lonsdale and M.N. de Pinho (Eds.), D. Reidal Publishing, (1986).

[70] Strathmann, H., "Production of microporous media by phase inversion processes", in *Materials Science of Synthetic Membranes*, D.R. Lloyd (Ed.), ACS, Washington, DC (1985), p165.

[71] Strathmann, H., C.M. Bell and K. Kimmerle, "Development of Synthetic membranes for gas and vapor separation", *Pure Appl. Chem.*, 58, 1663(1986).

[72] Takada, K., H. Matsuya, T. Masuda and H. Higashimura, "Gas permeability of polyacetylenes carrying substituents", *J. Appl. Polym. Sci.*, 30, 1605(1985).

[73] Torrey, S., *Membrane and Ultrafiltration Technology: Development Since 1981*, Noyes Data Corp., Park Ridge, NJ (1984).

[74] Van der Sheer, A. and J. Werner, "Plasma polymer membranes for gas separation: Development of three–layer membranes with a selective plasma polymer layer", *Proc. Int. Cong. Membrane*, Tokyo (1987), p518.

[75] Vieth, W.R., J.M. Howell and J.H. Hsieh, "Dual sorption theory", *J. Membrane Sci.*, 1, 177(1976).

[76] Vos, K.D. and F.O. Burris, Jr., "Drying cellulose acetate reverse osmosis membranes", *Ind. Eng. Chem. Prod. Res. Dev.*, 8, 84(1969).

[77] Ward, W.J., "Membrane gas separations – why and how", in *synthetic membranes: Science, Engineering and Applications*, P.E. Bungay, H.K. Lonsdale and M.N. de Pinho (Eds.), D. Reidel Publishing, (1986), p389.

[78] Ward, W.J., W.R. Browall and R.M. Salemme, "Ultrathin silicone – polycarbonate membranes for gas separation processes", *J. Membrane Sci.*, 1, 99(1976).

[79] Wijmans, J.G. and C.A. Smolders, "Preparation of asymmetric membranes by the phase inversion process", in *Synthetic Membranes: Science, Engineering and Applications*, P.M. Bungay, H.K. Lonsdale and M.N. de Pinho (Eds.), D. Reidal Publishing, (1986), p39.

[80] Zhu, C.L. and M.E. Liu, *Handbook of Membrane Processes*, Chemical Industry Press, Beijing (1988).

Appendix A
Derivation of Surface Flow Expression (Chen et al., 1989)

Consider a thin film of adsorbed gas layer (thickness t) moving on the surface of a cylindrical pore (radius r) in the axial direction at an average velocity of u.

Assuming a linear velocity profile in the direction vertical to the movement of the film (see Figure 2.1), the velocity gradient is $\frac{u}{(t/2)}$. Then, the shear stress working on the film is

$$-\mu\frac{u}{(t/2)}(2\pi r)\,dl$$

The spreading pressure working on the film $= -2\pi r\,d\phi$

Both forces have to be balanced to achieve a steady state movement of the film

$$-\mu\frac{u}{(t/2)}(2\pi r)\,dl - 2\pi r\,d\phi = 0 \tag{1}$$

Rearranging

$$d\phi = -\mu\frac{u}{(t/2)}\,dl \tag{2}$$

From isothermal equilibrium equation

$$RT\frac{dp}{p} = A_m\,d\phi \tag{3}$$

where A_m, the surface area per mole of adsorbed gas, is given by

$$A_m = \frac{2\pi r}{\overline{C}_{A,i}[\pi r^2 - \pi(r-t)^2]\,dl} = \frac{2r}{\overline{C}_{A,i}(2r-t)t} \tag{4}$$

where $\overline{C}_{A,i}$ is the average concentration of gas A at the interfacial adsorption layer.

Then, Eq.(3) becomes

$$RT\frac{dp}{p} = \frac{2r}{\overline{C}_{A,i}(2r-t)t}\,d\phi \tag{5}$$

Combining Eq.(2) and Eq.(5)

$$RT\frac{dp}{p} = -\frac{2r}{\overline{C}_{A,i}(2r-t)t}\,\mu\,\frac{u}{(t/2)}\,dl \tag{6}$$

Rearranging

$$u = -\frac{(2r-t)t^2}{4r}\,\frac{RT\overline{C}_{A,i}}{\mu}\,\frac{1}{p}\,\frac{dp}{dl} \tag{7}$$

Therefore, the mole flow rate of the gas through one pore is

$$\begin{aligned} q_s &= [\pi r^2 - \pi(r-t)^2]u\overline{C}_{A,i} \\ &= -\frac{\pi(2r-t)^2t^3}{4r}\,\frac{RT\overline{C}_{A,i}^2}{\mu}\,\frac{1}{p}\,\frac{dp}{dl} \end{aligned} \tag{8}$$

Assume $\overline{C}_{A,i}$ is proportional to p and the proportionality constant is k_H (the Henry's constant)

$$\overline{C}_{A,i} = k_H\,p \tag{9}$$

Eq.(8) becomes

$$q_s = -\frac{\pi(2r-t)^2t^3}{8r}\,\frac{RTk_H^2}{\mu}\,\frac{dp^2}{dl} \tag{10}$$

Approximating the derivative by $-\Delta(p^2)/l$

$$q_s = \frac{1}{l}\frac{\pi(2r-t)^2t^3}{8r}\frac{RT}{\mu}k_H^2\Delta(p^2) \tag{11}$$

where l is the length of the pore channel.

The gas permeation flux is therefore

$$Q_s = N_t q_s = \frac{N_t}{l}\frac{\pi(2r-t)^2t^3}{8r}\frac{RT}{\mu}k_H^2\Delta(p^2) \tag{12}$$

where N_t is the number of pores per unit membrane surface area.

Appendix B

Experimental Data of CO_2/CH_4 Mixtures Permeation Through Cellulose Acetate Membranes

Table B.1: Permeation Rates of CO_2/CH_4 Through Cellulose Acetate Membranes*

Operating Condition		[PR]**		Operating Condition		[PR]**	
Composition	Pressure	Film #1		Composition	Pressure	Film #2	
mole% CO_2	kPa	CO_2	CH_4	mole% CO_2	kPa	CO_2	CH_4
9.73	345	0.005	0.011	9.51	345	0.294	1.125
	689	0.012	0.024		689	0.624	2.394
	1034	0.030	0.024		1034	1.045	4.652
	1379	0.053	0.029		1379	1.419	5.989
	1724	0.081	0.039		1724	1.915	7.808
	2068	0.110	0.050		2068	2.213	9.970
20.30	345	0.012	0.010	21.80	345	0.585	0.941
	689	0.038	0.009		689	1.305	2.011
	1034	0.068	0.014		1034	2.110	3.508
	1379	0.112	0.022		1379	2.754	4.965
	1724	0.160	0.030		1724	3.542	6.672
	2068	0.185	0.033		2068	4.329	8.471
53.90	345	0.064	0.003	50.01	345	1.455	0.630
	689	0.147	0.006		689	3.445	1.313
	1034	0.349	0.014		1034	5.724	2.531
	1379	0.584	0.024		1379	7.249	3.452
	1724	0.839	0.033		1724	-	-
	2068	0.911	0.031		2068	-	-
78.93	345	0.234	0.003	78.70	345	2.805	0.271
	689	1.137	0.015		689	5.990	0.577
	1034	1.910	0.025		1034	9.599	0.989
	1379	2.525	0.035		1379	14.91	1.528
	1724	3.180	0.043		1724	20.80	2.181
	2068	3.250	0.039		2068	27.46	2.721
89.89	345	0.447	0.002	89.98	345	3.984	0.143
	689	1.518	0.008		689	8.381	0.299
	1034	2.555	0.013		1034	13.13	0.533
	1379	3.608	0.020		1379	18.87	0.758
	1724	4.255	0.025		1724	25.03	1.758
	2068	4.517	0.027		2068	-	-

*Pore radii on membrane surface: #1, 3.84Å; #2, 8.87Å;
**In 10^{-3}mol/m^2.s

Table B.2: Permeation Rates of CO_2/CH_4 Through Cellulose Acetate Membranes*

Operating Condition		Permeation Rate $\times 10^3$, mol/m^2.s					
Composition	Pressure	Film #3		Film #4		Film #5	
mole% CO_2	kPa	CO_2	CH_4	CO_2	CH_4	CO_2	CH_4
10.16	345	0.802	3.548	0.441	1.063	-	-
	689	1.201	7.516	0.526	1.649	1.702	12.15
	1034	1.802	11.95	0.765	2.663	2.511	19.31
	1379	2.297	16.69	0.998	3.846	3.234	43.51
	1724	2.903	21.61	1.186	5.506	4.344	45.47
	2068	3.481	26.26	1.375	6.285	5.339	56.95
21.80	345	1.100	3.136	0.427	0.699	-	-
	689	2.411	6.344	0.883	1.428	4.456	14.18
	1034	3.605	9.789	1.409	2.218	6.661	21.43
	1379	4.608	13.69	1.908	3.148	5.964	31.31
	1724	6.386	17.69	2.418	4.268	11.86	38.44
	2068	7.571	22.61	2.890	5.433	15.05	51.92
50.10	345	2.657	1.982	1.014	0.410	-	-
	689	5.317	4.003	2.067	0.843	9.224	8.210
	1034	8.045	6.197	3.265	1.321	14.02	12.95
	1379	11.46	8.762	4.689	1.899	19.41	18.05
	1724	15.14	10.95	6.137	2.469	24.49	22.54
	2068	18.98	14.18	7.702	2.998	34.87	28.92
78.70	345	4.482	0.897	1.940	0.202	-	-
	689	9.462	1.836	4.183	0.403	8.179	1.315
	1034	15.74	2.987	6.951	0.681	13.25	2.185
	1379	22.40	4.387	9.509	0.964	32.10	4.270
	1724	30.24	6.131	13.66	1.435	35.25	4.485
	2068	37.58	7.971	17.94	1.984	45.46	11.04
89.98	345	5.711	0.399	2.557	0.087	-	-
	689	11.42	0.835	5.189	0.175	16.02	1.493
	1034	17.74	1.340	7.991	0.264	27.54	2.648
	1379	25.99	2.102	12.23	0.407	48.01	4.661
	1724	36.23	2.666	16.15	0.560	53.50	4.952
	2068	44.80	3.584	20.41	0.762	65.42	6.296

*Pore radii on membrane surface: #3, 10.56Å; #4, 7.76Å; #5, 11.69Å.

Table B.3: Permeation Rates of CO_2/CH_4 Through Cellulose Acetate Membranes*

Operating Condition		Permeation Rate $\times 10^3$, mol/m^2.s			
Composition	Pressure	Film #6		Film #7	
mole% CO_2	kPa	CO_2	CH_4	CO_2	CH_4
9.51	345	0.032	0.043	0.012	0.035
	689	0.058	0.068	0.064	0.063
	1034	0.131	0.134	0.124	0.108
	1379	0.193	0.189	0.273	0.148
	1724	0.266	0.243	0.325	0.266
	2068	0.277	0.262	0.417	0.365
20.90	345	0.075	0.034	0.065	0.026
	689	0.190	0.072	0.174	0.055
	1034	0.343	0.119	0.298	0.089
	1379	0.524	0.176	0.406	0.062
	1724	0.661	0.223	0.413	0.127
	2068	0.773	0.258	0.680	0.214
56.90	345	0.178	0.013	0.051	0.004
	689	0.420	0.027	0.330	0.015
	1034	0.736	0.045	0.378	0.020
	1379	1.045	0.063	0.656	0.035
	1724	1.378	0.082	0.918	0.051
	2068	1.775	0.107	1,160	0.065
76.80	345	0.583	0.012	-	-
	689	1.284	0.025	-	-
	1034	2.560	0.049	-	-
	1379	3.558	0.070	-	-
	1724	4.481	0.090	-	-
	2068	4.981	0.107	-	-
88.80	345	0.880	0.007	0.047	0.004
	689	2.531	0.021	1.269	0.014
	1034	3.697	0.031	1.392	0.023
	1379	5.012	0.044	1.695	0.025
	1724	6.346	0.054	2.756	0.028
	2068	7.593	0.068	3.054	0.039

*Pore radii on membrane surface: #6, 4.77Å; #7, 4.92Å.

Appendix C

Experimental Results for Permselectivity of Polyimide Membranes

Table C.1: Permeabilities of organic vapors and air through a polyimide membrane at 22.5°C

Organic Vapor	Permeability, J_{vap} mol/m^2.s.Pa	Selectivity J_{vap}/J_{air}
Methanol	1.32×10^{-8}	378.5
Ethanol	1.81×10^{-8}	517.7
Acetone	4.89×10^{-9}	141.1
Benzene	5.46×10^{-9}	156.2
Toluene	1.95×10^{-8}	558.9
p–Xylene	4.65×10^{-8}	1336.0
m–Xylene	5.22×10^{-8}	1498.1
1,2–Dichloroethane	4.25×10^{-9}	121.9
1,2–Dichloropropane	8.14×10^{-9}	233.4
Chloroform	2.15×10^{-9}	61.6
Carbon tetrachloride	2.30×10^{-9}	65.7
Hexane	1.93×10^{-9}	55.2
Air permeability $J_{air} = 3.49 \times 10^{-11}$ mol/m^2.s.Pa		

Membrane making conditions

Casting solution: PI 25wt% + LiCl 2.5wt% + DMAc 72.5wt%

Evaporation temperature: 85°C

Evaporation period: 20min

Gelation medium: ice cold water

Gelation period: 20min

Table C.2: Permeabilities of organic vapors and air through a polyimide membrane at 22.5°C

Organic Vapor	Permeability, J_{vap} mol/m^2.s.Pa	Selectivity J_{vap}/J_{air}
Methanol	5.02×10^{-8}	221.2
Ethanol	6.73×10^{-8}	296.9
Acetone	1.07×10^{-8}	47.4
Benzene	1.15×10^{-8}	50.5
Toluene	4.09×10^{-8}	179.9
p–Xylene	1.04×10^{-8}	460.2
m–Xylene	1.16×10^{-7}	513.3
1,2–Dichloroethane	1.18×10^{-8}	52.1
1,2–Dichloropropane	1.30×10^{-8}	57.2
Chloroform	4.79×10^{-9}	21.1
Carbon tetrachloride	5.56×10^{-9}	24.4
Hexane	7.33×10^{-9}	32.4
Air permeability $J_{air} = 2.27 \times 10^{-10}$ mol/m^2.s.Pa		

Membrane making conditions

Casting solution: PI 25wt% + LiCl 3.6wt% + DMAc 71.4wt%

Evaporation temperature: 85°C

Evaporation period: 20min

Gelation medium: ice cold water

Gelation period: 20min

Table C.3: Permeabilities of organic vapors and air through a polyimide membrane at 22.5°C

Organic Vapor	Permeability, J_{vap} mol/m^2.s.Pa	Selectivity J_{vap}/J_{air}
Methanol	1.21×10^{-7}	268.6
Ethanol	1.52×10^{-7}	338.5
Acetone	3.31×10^{-8}	73.8
Benzene	3.89×10^{-8}	86.2
Toluene	1.37×10^{-7}	304.7
p–Xylene	3.87×10^{-7}	860.1
m–Xylene	3.97×10^{-7}	881.2
1,2–Dichloroethane	4.52×10^{-8}	100.7
1,2–Dichloropropane	6.68×10^{-8}	149.1
Chloroform	1.35×10^{-8}	30.0
Carbon tetrachloride	1.88×10^{-8}	41.8
Hexane	2.61×10^{-8}	58.0
Air permeability $J_{air} = 4.50 \times 10^{-10}$ mol/m^2.s.Pa		

Membrane making conditions

Casting solution: PI 25wt% + LiCl 5wt% + DMAc 70wt%

Evaporation temperature: 85°C

Evaporation period: 20min

Gelation medium: ice cold water

Gelation period: 20min

Table C.4: Permeabilities of organic vapors and air through a polyimide membrane at 22.5°C

Organic Vapor	Permeability, J_{vap} mol/m^2.s.Pa	Selectivity J_{vap}/J_{air}
Methanol	1.49×10^{-7}	139.1
Ethanol	2.88×10^{-7}	270.0
Acetone	4.72×10^{-8}	44.2
Benzene	7.53×10^{-8}	70.5
Toluene	2.63×10^{-7}	245.1
p–Xylene	4.35×10^{-7}	407.6
m–Xylene	4.99×10^{-7}	467.4
1,2–Dichloroethane	5.66×10^{-8}	53.0
1,2–Dichloropropane	7.47×10^{-8}	69.9
Chloroform	2.30×10^{-8}	21.6
Carbon tetrachloride	2.23×10^{-8}	20.8
Hexane	5.46×10^{-8}	51.1
Air permeability $J_{air} = 1.07 \times 10^{-9}$ mol/m^2.s.Pa		

Membrane making conditions

Casting solution: PI 25wt% + LiCl 3.6wt% + DMAc 71.4wt%

Evaporation temperature: 55°C

Evaporation period: 20min

Gelation medium: ice cold water

Gelation period: 20min

Table C.5: Permeabilities of organic vapors and air through a polyimide membrane at 22.5°C

Organic Vapor	Permeability, J_{vap} mol/m^2.s.Pa	Selectivity J_{vap}/J_{air}
Methanol	9.84×10^{-8}	207.2
Ethanol	1.35×10^{-7}	284.7
Acetone	1.77×10^{-8}	37.2
Benzene	3.04×10^{-8}	63.9
Toluene	1.23×10^{-7}	259.3
p–Xylene	2.24×10^{-7}	472.2
m–Xylene	2.40×10^{-7}	506.0
1,2–Dichloroethane	3.75×10^{-8}	78.9
1,2–Dichloropropane	4.66×10^{-8}	98.5
Chloroform	1.88×10^{-8}	39.7
Carbon tetrachloride	1.96×10^{-8}	41.3
Hexane	2.38×10^{-8}	50.2
Air permeability $J_{air} = 4.74 \times 10^{-10}$ mol/m^2.s.Pa		

Membrane making conditions

Casting solution: PI 25wt% + LiCl 3.6wt% + DMAc 71.4wt%

Evaporation temperature: 65°C

Evaporation period: 20min

Gelation medium: ice cold water

Gelation period: 20min

Table C.6: Permeabilities of organic vapors and air through a polyimide membrane at 22.5°C

Organic Vapor	Permeability, J_{vap} mol/m^2.s.Pa	Selectivity J_{vap}/J_{air}
Methanol	1.31×10^{-8}	193.7
Ethanol	1.44×10^{-8}	213.6
Acetone	2.25×10^{-9}	33.3
Benzene	3.01×10^{-9}	44.6
Toluene	1.97×10^{-8}	292.8
p–Xylene	3.19×10^{-8}	473.4
m–Xylene	3.28×10^{-8}	487.3
1,2–Dichloroethane	3.98×10^{-9}	59.4
1,2–Dichloropropane	3.97×10^{-9}	59.1
Chloroform	1.67×10^{-9}	24.9
Carbon tetrachloride	2.31×10^{-9}	34.3
Hexane	2.39×10^{-9}	35.4
Air permeability $J_{air} = 6.74 \times 10^{-11}$ mol/m^2.s.Pa		

Membrane making conditions

Casting solution: PI 25wt% + LiCl 3.6wt% + DMAc 71.4wt%

Evaporation temperature: 110°C

Evaporation period: 20min

Gelation medium: ice cold water

Gelation period: 20min

Table C.7: Permeabilities of organic vapors and air through a polyimide membrane at 22.5°C

Organic Vapor	Permeability, J_{vap} mol/m^2.s.Pa	Selectivity J_{vap}/J_{air}
Methanol	1.16×10^{-7}	152.6
Ethanol	1.32×10^{-7}	173.9
Acetone	2.63×10^{-8}	34.7
Benzene	5.32×10^{-8}	70.3
Toluene	1.13×10^{-7}	148.7
p–Xylene	3.24×10^{-7}	427.8
m–Xylene	3.79×10^{-7}	501.2
1,2–Dichloroethane	4.55×10^{-8}	60.1
1,2–Dichloropropane	6.50×10^{-8}	85.8
Chloroform	1.64×10^{-8}	21.7
Carbon tetrachloride	2.40×10^{-8}	31.6
Hexane	2.66×10^{-8}	35.1
Air permeability $J_{air} = 7.59 \times 10^{-10}$ mol/m^2.s.Pa		

Membrane making conditions

Casting solution: PI 25wt% + LiCl 3.6wt% + DMAc 71.6wt%

Evaporation temperature: 85°C

Evaporation period: 5min

Gelation medium: ice cold water

Gelation period: 20min

Table C.8: Permeabilities of organic vapors and air through a polyimide membrane at 22.5°C

Organic Vapor	Permeability, J_{vap} mol/m^2.s.Pa	Selectivity J_{vap}/J_{air}
Methanol	7.30×10^{-8}	107.4
Ethanol	1.28×10^{-7}	188.6
Acetone	2.29×10^{-8}	33.7
Benzene	3.52×10^{-8}	51.7
Toluene	9.44×10^{-8}	138.9
p–Xylene	2.65×10^{-7}	389.6
m–Xylene	2.86×10^{-7}	421.2
1,2–Dichloroethane	3.05×10^{-8}	44.8
1,2–Dichloropropane	3.55×10^{-8}	52.2
Chloroform	1.18×10^{-8}	17.4
Carbon tetrachloride	1.58×10^{-8}	23.2
Hexane	2.32×10^{-8}	34.1
Air permeability $J_{air} = 6.79 \times 10^{-10}$ mol/m^2.s.Pa		

Membrane making conditions

Casting solution: PI 25wt% + LiCl 3.6wt% + DMAc 71.6wt%

Evaporation temperature: 85°C

Evaporation period: 10min

Gelation medium: ice cold water

Gelation period: 20min

Table C.9: Permeabilities of organic vapors and air through a polyimide membrane at 22.5°C

Organic Vapor	Permeability, J_{vap} mol/m^2.s.Pa	Selectivity J_{vap}/J_{air}
Methanol	1.95×10^{-8}	131.1
Ethanol	2.85×10^{-8}	191.8
Acetone	5.46×10^{-9}	36.8
Benzene	1.17×10^{-8}	79.0
Toluene	2.57×10^{-8}	173.6
p–Xylene	7.84×10^{-8}	528.2
m–Xylene	9.11×10^{-8}	614.1
1,2–Dichloroethane	8.57×10^{-9}	57.8
1,2–Dichloropropane	1.21×10^{-8}	81.5
Chloroform	3.28×10^{-9}	22.1
Carbon tetrachloride	4.75×10^{-9}	32.1
Hexane	5.16×10^{-9}	34.5
Air permeability $J_{air} = 1.48 \times 10^{-10}$ mol/m^2.s.Pa		

Membrane making conditions

Casting solution: PI 25wt% + LiCl 3.6wt% + DMAc 71.4wt%

Evaporation temperature: 85°C

Evaporation period: 30min

Gelation medium: ice cold water

Gelation period: 20min

Table C.10: Permeabilities of organic vapors and air through a polyimide membrane at 22.5°C

Organic Vapor	Permeability, J_{vap} mol/m^2.s.Pa	Selectivity J_{vap}/J_{air}
Acetone	2.50×10^{-9}	145
m–Xylene	2.33×10^{-8}	1350
Air permeability $J_{air} = 1.72 \times 10^{-11}$ mol/m^2.s.Pa		

Membrane making conditions

Casting solution: PI 25wt% + LiCl 1.25wt% + DMAc 73.75wt%
Evaporation temperature: 85°C
Evaporation period: 20min
Gelation medium: ice cold water
Gelation period: 20min

Table C.11: Permeabilities of organic vapors and air through a polyimide membrane at 22.5°C

Organic Vapor	Permeability, J_{vap} mol/m^2.s.Pa	Selectivity J_{vap}/J_{air}
Acetone	4.22×10^{-8}	7.1
m–Xylene	6.20×10^{-7}	96.0
Air permeability $J_{air} = 6.40 \times 10^{-9}$ mol/m^2.s.Pa		

Membrane making conditions

Casting solution: PI 25wt% + LiCl 5.75wt% + DMAc 69.25wt%
Evaporation temperature: 85°C
Evaporation period: 20min
Gelation medium: ice cold water
Gelation period: 20min

Table C.12: Permeabilities of organic vapors and air through a polyimide membrane at 22.5°C

Organic Vapor	Permeability, J_{vap} mol/m^2.s.Pa	Selectivity J_{vap}/J_{air}
Acetone	1.51×10^{-10}	32.0
m-Xylene	2.15×10^{-9}	458.1
Air permeability $J_{air} = 4.71 \times 10^{-12}$ mol/m^2.s.Pa		

Membrane making conditions

Casting solution: PI 25wt% + LiCl 3.6wt% + DMAc 71.4wt%

Evaporation temperature: 140°C

Evaporation period: 20min

Gelation medium: ice cold water

Gelation period: 20min

Table C.13: Permeabilities of organic vapors and air through a polyimide membrane at 22.5°C

Organic Vapor	Permeability, J_{vap} mol/m^2.s.Pa	Selectivity J_{vap}/J_{air}
Acetone	4.18×10^{-9}	43.4
m-Xylene	6.02×10^{-8}	624.1
Air permeability $J_{air} = 9.65 \times 10^{-11}$ mol/m^2.s.Pa		

Membrane making conditions

Casting solution: PI 25wt% + LiCl 3.6wt% + DMAc 71.4wt%

Evaporation temperature: 85°C

Evaporation period: 40min

Gelation medium: ice cold water

Gelation period: 20min

Table C.14: Permeabilities of organic vapors and air through a polyimide membrane at 22.5°C

Organic Vapor	Permeability, J_{vap} mol/m^2.s.Pa	Selectivity J_{vap}/J_{air}
Acetone	2.35×10^{-9}	45
m–Xylene	3.34×10^{-8}	642
Air permeability $J_{air} = 5.23 \times 10^{-11}$ mol/m^2.s.Pa		

Membrane making conditions

Casting solution: PI 25wt% + LiCl 3.6wt% + DMAc 71.4wt%

Evaporation temperature: 85°C

Evaporation period: 50min

Gelation medium: ice cold water

Gelation period: 20min